PHILOSOPHICAL TRANSACTIONS OF THE ROYAL SOCIETY A MATHEMATICAL, PHYSICAL & ENGINEERING SCIENCES

On the inverse fractal problem for two–dimensional attractors

A. Deliu, J. Geronimo and R. Shonkwiler

Phil. Trans. R. Soc. Lond. A 1997 **355**, 1017-1062
doi: 10.1098/rsta.1997.0052

On the inverse fractal problem for two-dimensional attractors

By A. Deliu, J. Geronimo and R. Shonkwiler

School of Mathematics, Georgia Institute of Technology, Atlanta, GA 30332, USA
(shenk@math.gatech.edu)

Contents

We give a theoretical, geometric solution of the inverse fractal problem for a large class of two-dimensional attractors which we call polyhulled disjoint (PHD) attrac-

Phil. Trans. R. Soc. Lond. A (1997) **355**, 1017–1062
Printed in Great Britain

tors. These are attractors of iterated function systems (IFS) with affine maps and range over a wide spectrum of shapes, both abstract and natural. Encoding the objects of a two-dimensional image in terms of their IFS results in enormous data compression.

Given a PHD attractor we present an algorithm to find its IFS code by performing a geometric analysis based on the extreme points theorem. We introduce an edge detection device, the springbar function, to extract the affine orbits entangled inside the attractor and then use the elementary properties of these orbits to determine the mappings which generated them.

Our solution is amenable to numerical implementation.

1. Introduction

We use the term *fractal* in the sense of Barnsley (1988), as a set generated by an iterated function system (IFS). An *iterated function system* $\mathcal{W}$ is a finite set of contractive affine maps $w_i : X \to X$, $i = 1, 2, \ldots, N$, defined on a compact metric space X to itself. Associated with an IFS is a unique subset $A = A(\mathcal{W})$ of X, the *attractor* of $\mathcal{W}$, which is characterized by the *tiling property* (Hutchinson 1981),

$$A = \bigcup_{i=1}^{N} w_i(A). \tag{1.1}$$

The sets $w_i(A)$ are the *tiles* of A (relative to $\mathcal{W}$) and the maps w_i their *generators*. Letting C_A denote the convex hull of A, the *first level tiles* or *hull tiles* of A relative to $\mathcal{W}$ are the sets $w_i(C_A)$, $i = 1, \ldots, N$. The existence of A can be demonstrated by realizing it as the fixed point under the set map, $\boldsymbol{W}(B) = \bigcup_{i=1}^{N} w_i(B)$, which is a contraction in the space of non-empty compact subsets of X under the Hausdorff metric (Barnsley 1988). Our principal interest here is with two-dimensional attractors and consequently X will be taken as the unit square of $\boldsymbol{R}^2$. By appropriate scaling, an arbitrary two-dimensional attractor can be realized as a subset of this square. Hence in what follows, each map w is of the form $w = W + \boldsymbol{b}$, where W is a 2×2 matrix and $\boldsymbol{b}$ is a two-dimensional vector. The constant map, $w\boldsymbol{x} = \boldsymbol{b}$ for all $\boldsymbol{x}$, can be used only to insert individual points at arbitrary places in the attractor. We will not consider such attractors. Similarly, we will not consider attractors resulting from iterated functions systems containing singular maps. Most, if not all, of our results continue to hold for non-constant singular maps but a great many new cases result from their consideration which we leave for the reader.

We also consider one-dimensional attractors. An IFS of one-dimensional maps, $\hat{w}(x) = sx + b$, may be embedded in the class of two-dimensional iterated function systems in many ways, for example by setting

$$w(\boldsymbol{x}) = \begin{pmatrix} s & 0 \\ 0 & s \end{pmatrix} \begin{pmatrix} x \\ y \end{pmatrix} + \begin{pmatrix} b \\ b \end{pmatrix}.$$

The diagonal of the square of the resulting two-dimensional attractor is a root two enlarged replica of the original one-dimensional attractor.

Attractors may be graphically rendered to produce wonderfully detailed monochrome images on a computer screen or the printed page. The fractal shrub

of figure 7 is such an example. By adjusting the generating maps of an IFS, the resulting image may be controlled and can have an appearance ranging from classical geometric objects, to natural objects, to highly abstract objects with fractal dimension not equal to the topological dimension (Mandelbrot 1982). The *forward problem* of fractal geometry is that of rendering the attractor of a given IFS.

Conversely, the *inverse problem* of fractal geometry is that of determining the IFS maps which produce a given attractor. The problem has been previously studied, frequently in the more general context of invariant measures on fractals (Abenda & Turchetti 1989; Barnsley *et al.* 1985; Cabrelli *et al.* 1992*a*, *b*; Diaconis & Shahshahani 1986; Handy & Mantica 1990; Mantica & Sloan 1989; Vrscay & Roehrig 1989; Vrscay 1990, 1991*a*, *b*; Bessis & Demko 1990; Strichartz 1993). Most of these papers treat the one-dimensional case using the theory of moments of measures. However, up to now, the numerical implementation of the moment approach has proved impratical.

In this work we present an entirely different approach to solving the inverse problem, one that is geometrically based. Our methods can be applied to a reasonably large class of one- and two-dimensional attractors which moreover are important in image applications, the class of polyhulled disjoint attractors (PHD attractors). This class includes those shown in figures 14–16. We formally define them in § 2. (The method also applies to figures 10–13 as these are 'essentially disjoint'.) Given an attractor A of this class we show how to find a $\mathcal{W}$ so that $A = A(\mathcal{W})$ exactly. In § 2 we also introduce refinement IFSs and the extreme points theorem, the principal result on which our work is based. This leads to the notion of formative and decorative tiles.

Our method also makes use of the elementary properties of the orbits of points under affine contractions. The *orbit* of a point $\boldsymbol{x}$ under the map w is the sequence of iterates $w^k(\boldsymbol{x})$, $k = 0, 1, \ldots$. In § 3 we detail the correspondence between the eigenvalues and eigenvectors of a formative map and geometrical features of its trajectories, a continuous version of an orbit. This leads to the notion of natural coordinate systems. In § 4 we express these salient features in terms of polar coordinates based at the extreme point under study.

A major obstacle in our approach to solving the inverse problem is that the orbits of all the points of an attractor are mixed together and must be disentangled. In § 5 we introduce a certain edge or margin tracking tool, the *springbar function*, for this purpose and for eliciting the geometrical properties of trajectories. In § 6 we introduce the *gap analysis* for recovering the multiplicative periodicity of an orbit which was lost in its trajectory and enabling the calculation of the eigenvalues associated with a trajectory.

Ultimately the main task is that of distinguishing among several cases classified by eigenvalues. As each tool is introduced, we detail its application to each spectral case.

In § 7 we show how to calculate the encoding of decorative tiles. Again our approach is based on spectral methods.

Actually our geometrical method works for attractors beyond the class of polyhulled disjoint ones, for example on attractors all of whose tiles have finitely many extreme points (disjoint or not), such as the fractal shrub. Further, by adding limiting techniques, the subject of § 8, the class which may be inverted expands to include just touching (see § 2) polyhulled attractors as well, such as the dragon attractor (see figure 9). Moreover if only approximate solutions are required, the Collage theorem (Barnsley *et al.* 1985), which states, roughly, that *the better an image can be tiled*

by affine copies of itself, the closer will be the attractor of the resulting IFS to the image, suggests that the class of solvable images can be greatly expanded although we have not investigated this.

A major unfinished extension of the work, which the authors believe is possible, is to non-polyhulled attractors such as the black spleenwort fern (see figure 8).

While the primary interest here is in the theoretical solution of the inverse problem, our geometrical method is amendable to numerical implementation. As has been previously noted, IFS encoding results in enormous data compression and hence significant commerical value (Barnsley & Sloan 1985).

(*a*) *Summary of the method*

1. At each extreme point $\boldsymbol{p}$ of the convex hull C_A of A perform a springbar analysis to obtain sufficient parameter information enabling the calculation of trajectory maps at $\boldsymbol{p}$.

2. Using the trajectory maps, calculate the domain of invariance and supporting trajectories at each extreme point. Distinguish primary versus secondary extreme points.

3. With the trajectory maps at $\boldsymbol{p}$ in hand, for each $\boldsymbol{x}$ in the domain of invariance at $\boldsymbol{p}$, perform a gap analysis on the fractal dust corresponding to the trajectory through $\boldsymbol{x}$ to calculate its multiplicative period, $\lambda_{\boldsymbol{x}}$.

4. Using the collection of spectra $\lambda_{\boldsymbol{x}}$, calculate the minor eigenvalue and hence the locally formative map at $\boldsymbol{p}$. This solves primary maps; it remains to solve secondary maps.

5. By matching spectra, determine the primary pre-image for each secondary extreme point. By matching respective supporting trajectories calculate each secondary decorative map; it remains to calculate interior decorative maps.

6. By means of fat-curves, well order interior tiles. Using the same techniques as for secondary points above, successively solve, and colour, the interior tiles until the entire attractor is coloured.

2. The class of disjoint polyhulled attractors

(*a*) *Equivalence classes of IFSs*

It is well known, and easy to show by example, that distinct iterated function systems can have identical attractors. (We do not regard a permutation of the maps of an IFS as constituting a distinct one.) For example, if the attractor has symmetries, groups of transformations, invariant under the particular symmetry, can be used to construct equivalent systems.

Let $\mathcal{E}(A)$ denote the class of all iterated function systems whose attractor is A,

$$\mathcal{E}(A) = \{\mathcal{W} : A(\mathcal{W}) = A\},$$

or $\mathcal{E}(A) = \emptyset$ if A is not the attractor of any IFS.

Definition 2.1. *We say an affine map w is invariant for the attractor A if $w(A) \subset A$.*

Evidently any invariant map can be added to an IFS and the result will again be an IFS for the same attractor. Conversely, it may be possible to remove one or more maps from an IFS without affecting its attractor. We define the index of A to be the

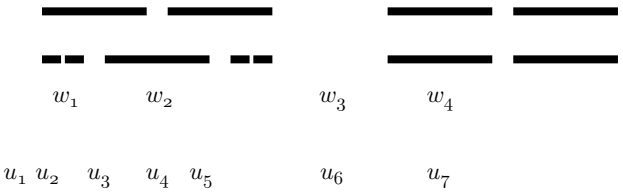

Figure 1. First level tiles of the partial refinement example.

smallest number of maps which will generate the attractor A,

$$\text{index}(A) = \min\{\text{card}(\mathcal{W}) : \mathcal{W} \in \mathcal{E}(A)\}.$$

If $\mathcal{W} = \{w_1, \ldots, w_N\}$ is an IFS for A, then the compositions $w_1 \circ w_i(A)$, $i = 1, \ldots, N$, subtile $w_1(A)$. Hence

$$w_1\mathcal{W} = \{w_1 \circ w_1 \circ w_1^{-1}, w_1 \circ w_2 \circ w_1^{-1}, \ldots, w_1 \circ w_N \circ w_1^{-1}\}$$

is an IFS for $w_1(A)$.

More generally, let $\mathcal{W}$ and $\mathcal{W}'$ be two iterated function systems for an attractor A. We say $\mathcal{W}'$ is a *refinement* of $\mathcal{W}$ if every tile $w'(A)$ of $\mathcal{W}'$ is contained in some tile of $\mathcal{W}$, that is $w'(A) \subset w(A)$, for some $w \in \mathcal{W}$. Given iterated function systems $\mathcal{W}_1, \mathcal{W}_2 \in \mathcal{E}(A)$, with $N_k = \text{card}(\mathcal{W}_k)$, $k = 1, 2$, one of their *common refinements*, $\mathcal{W} = \mathcal{W}_1 \circ \mathcal{W}_2$, is the set of all compositions

$$\mathcal{W} = \{w_i^1 \circ w_j^2 \,:\, w_i^1 \in \mathcal{W}_1, w_j^2 \in \mathcal{W}_2\}.$$

Since $\mathcal{W}_2$ induces a tiling of A, it follows that $w_i^1 \circ w_j^2(A) \subset A$, $i = 1, \ldots, N_1$, $j = 1, \ldots, N_2$, and

$$\bigcup_{j=1}^{N_2} w_i^1 \circ w_j^2(A) = w_i^1\left(\bigcup_{j=1}^{N_2} w_j^2(A)\right) = w_i^1(A). \tag{2.1}$$

Hence

$$\bigcup_{i=1}^{N_1}\bigcup_{j=1}^{N_2} w_i^1 \circ w_j^2(A) = A$$

showing that $\mathcal{W} \in \mathcal{E}(A)$. Of course the same holds for their other common refinement $\mathcal{W}_2 \circ \mathcal{W}_1$. This proves the following.

Proposition 2.2. *Let $\mathcal{W}_1, \mathcal{W}_2 \in \mathcal{E}(A)$, then also the refinement $\mathcal{W}_1 \circ \mathcal{W}_2 \in \mathcal{E}(A)$.*

Equation (2.1) also shows that each tile $w_i^1(A)$ of $\mathcal{W}_1$ is itself *subtiled* by the $\mathcal{W}_2$ tiles $w_i^1 \circ w_j^2(A)$, in a manner similar to the tiling of A by $\mathcal{W}_2$. Thus each tile of the common refinement $\mathcal{W}$ is either disjoint from or wholly contained in each tile of its second argument $\mathcal{W}_1$.

Remarks 2.1. It is possible that for two iterated function systems having the same attractor, the tiles of one only partially refine tiles of the other. This occurs for the one-dimensional attractor due to the following two iterated function systems (see figure 1; this example is due to George Donovan):

$$\mathcal{W} = \left\{w_1(x) = \frac{2}{11}x, \quad w_2(x) = \frac{2}{11}x + \frac{12}{55}, \quad w_3(x) = \frac{2}{11}x + \frac{3}{5}, \quad w_4(x) = \frac{2}{11}x + \frac{9}{11}\right\}$$

and

$$\mathcal{U} = \Big\{ u_1(x) = \frac{4}{121}x, \quad u_2(x) = \frac{4}{121}x + \frac{24}{605}, \quad u_3(x) = \frac{2}{11}x + \frac{6}{55},$$
$$u_4(x) = \frac{4}{121}x + \frac{18}{55}, \quad u_5(x) = \frac{4}{121}x + \frac{222}{605}, \quad u_6 = w_3, \quad u_7 = w_4 \Big\}.$$

Obviously a common refinement may be further subtiled by yet another equivalent IFS for its attractor. In particular we may take $\mathcal{W}_2$ above to be $\mathcal{W}_1$ in which case we write

$$\mathcal{W}_1^2 = \mathcal{W}_1 \circ \mathcal{W}_1.$$

More generally, the *power refinements* of $\mathcal{W}$ are, for some k,

$$\begin{aligned} \mathcal{W}^k &= \mathcal{W} \circ \ldots \circ \mathcal{W}, \qquad k \text{ times} \\ &= \{ w_{i_1} \circ w_{i_2} \circ \ldots \circ w_{i_k} : w_{i_j} \in \mathcal{W}, \qquad j = 1, \ldots, k \}. \end{aligned}$$

(*b*) *Disjoint attractors*

Definition 2.3. *An IFS $\mathcal{W}$ is disjoint if its tiles are pairwise disjoint, $w_i(A) \cap w_j(A) = \emptyset$, for $1 \leqslant i < j \leqslant N$. An attractor A is disjoint if it has at least one disjoint IFS, that is $\mathcal{W}$ is disjoint for some $\mathcal{W} \in \mathcal{E}(A)$.*

The following is an elementary observation stemming from the compactness of tiles.

Proposition 2.4. *Given a disjoint IFS $\mathcal{W}$ for A, there exist $\delta > 0$ such that*

$$\operatorname{dist}(w_i(A), w_j(A)) \geqslant \delta \qquad \text{for all } w_i, w_j \in \mathcal{W},\ i \neq j.$$

Corollary 2.5. *Let A be a disjoint attractor and $w_1(A)$ and $w_2(A)$ be two distinct tiles for some disjoint $\mathcal{W} \in \mathcal{E}(A)$. Let $\boldsymbol{x}(t)$, $a \leqslant t \leqslant b$, be a curve in $\boldsymbol{R}^2$ such that $\boldsymbol{x}(a) \in w_1(A)$ and $\boldsymbol{x}(b) \in w_2(A)$. Then for some interval $t \in (c, d)$, $\boldsymbol{x}(t) \cap A = \emptyset$.*

Proposition 2.6. *Let $\mathcal{W}_1$ and $\mathcal{W}_2$ be disjoint IFSs for A. Then their common refinements are also disjoint.*

Proof. Let $\mathcal{W}_k = \{w_1^k, w_2^k, \ldots\}$, $k = 1, 2$. By symmetry it suffices to consider $\mathcal{W}_1 \circ \mathcal{W}_2$. If $i \neq j$ then $w_i^k(S) \cap w_j^k(S) = \emptyset$, $k = 1, 2$, for any $S \subset A$. Hence if either $i \neq k$ or $j \neq m$ then

$$w_i^1 \circ w_j^2(A) \cap w_k^1 \circ w_m^2(A) = \emptyset.$$

■

Definition 2.7. *An attractor A is said to be just touching if it has an IFS $\mathcal{W}$ satisfying the open set condition and $w_i(A) \cap w_j(A) \neq \emptyset$ for some generators $w_i \neq w_j$. The open set condition holds for $\mathcal{W}$ if there exists a non-empty open set $\mathcal{O}$ such that $w_i(\mathcal{O}) \cap w_j(\mathcal{O}) = \emptyset$, for all $i \neq j$, and $\bigcup_i w_i(\mathcal{O}) \subset \mathcal{O}$ (cf. Hutchinson 1981).*

(*c*) *The convex hull and its extreme points*

Given a line ℓ in the plane, $\ell = \{(x, y) : ax + by = c\}$, where $a, b, c \in \boldsymbol{R}$, $ab \neq 0$, let $J_\ell = \{(x, y) : ax + by \geqslant c\}$ be the closed half space consisting of ℓ itself and its open 'positive' half space. We say ℓ *supports* a set S if $S \subset J_\ell$ and $\bar{S} \cap \ell \neq \emptyset$. We say

$\boldsymbol{p} \in S$ is an *extreme point* of S if $\boldsymbol{p}$ belongs to at least two distinct supporting lines of S. Let $\mathrm{ext}(S)$ denote the set of extreme points of S.

Let A be an attractor, its *convex hull*, C_A, is the intersection of all closed half-spaces containing A,

$$C_A = \bigcap_{\ell \in L} J_\ell,$$

where $\ell \in L$ if and only if $A \subset J_\ell$. Evidently C_A is closed and is the smallest convex set which contains A. We orient the boundary of the convex hull as usual, counterclockwise. If A is the attractor of an IFS, then A is compact and thus C_A is a compact convex set.

Definition 2.8. *An IFS is strongly disjoint if $w_i(C_A) \cap w_j(C_A) = \emptyset$ for all $i \neq j$ where C_A is the convex hull of A. Likewise, an attractor A is strongly disjoint if it has a strongly disjoint IFS. Figure 14 shows a disjoint but not strongly disjoint gasket type attractor.*

It is obvious that proposition 2.6 continues to hold for strongly disjoint attractors.

Definition 2.9. *An affine map w is k-invertible for an attractor A if it is invariant for A and for every $\boldsymbol{x} \in w^k(C_A) \cap A$; $w^{-1}(\boldsymbol{x}) \in A$; w is invertible if it is k-invertible for $k = 1$. An IFS is invertible if every one of its maps is.*

Theorem 2.10. *If $\mathcal{W}$ is a strongly disjoint IFS for A, then $\mathcal{W}$ is invertible.*

Proof. Since $w(C_A) \supset w(A)$, this follows easily from (1.1). ■

Theorem 2.11. *If $\mathcal{W}$ is a disjoint IFS for A and $w \in \mathcal{W}$, then w is k-invertible for A for some $k = 1, 2, \ldots$.*

Proof. Since the $w_i(A)$, $w_i \in \mathcal{W}$, are disjoint compact sets, there is a $\delta > 0$ such that the set distance between every (distinct) pair of sets $w_i(A)$ and $w_j(A)$, $w_i, w_j \in \mathcal{W}$, exceeds δ. Now let k be sufficiently large that $\mathrm{diam}(w^k(A)) < \delta$. Then by (1.1), if $\boldsymbol{x} \in w^k(C_A) \cap A$, it follows that $\boldsymbol{x}$ can not lie in $w_i(A)$ for $w_i \neq w$. Hence $\boldsymbol{x} \in w(A)$ and so $w^{-1}(\boldsymbol{x}) \in A$. ■

Corollary 2.12. *With k as in the theorem, if $\boldsymbol{x} \in w^{k+n}(C_A) \cap A$, $n \geqslant 0$, then $w^{-i}(\boldsymbol{x}) \in A$ for $1 \leqslant i \leqslant n$. If G is an open subset of $w^k(C_A)$ disjoint from A, i.e. a gap in A, then $w^{k+n}(G)$ is a gap in A for all $n \geqslant 0$.*

Definition 2.13. *An attractor A is flat if for some line ℓ, $A \subset \ell$. Obviously a flat attractor has exactly two extreme points and its convex hull consists of a line segment.*

The following result is central to our work.

Theorem 2.14. (Extreme points) *Let A be the attractor of an iterated function system $\mathcal{W}$. Then every extreme point $\boldsymbol{p}$ of A is the image of an extreme point $\boldsymbol{q}$ of A under some generating map, that is*

$$\mathrm{ext}(A) \subset \bigcup_{i=1}^{N} w_i(\mathrm{ext}(A)).$$

Proof. See Berger (1991). ■

The theorem allows, and it often occurs, that an extreme point $\boldsymbol{p}$ is the image of itself under a generating map. This is a sufficiently important case to warrant a definition.

Definition 2.15. *An invariant map w for A is formative if its fixed point is also an extreme point of A, otherwise it is decorative. An extreme point $\boldsymbol{p}$ is a primary point or an extreme fixed point if it is the fixed point of some formative map, otherwise it is secondary.*

Remarks 2.2. A single tile can have more than one extreme point, even if one of these is an extreme fixed point (see gasketflip, figure 13). It is also possible that no extreme point is primary for a given IFS (see dragontails, figure 10); however, we will show below that there always exists an equivalent IFS for every polyhulled disjoint attractor in which at least one extreme point is primary and moreover in which every secondary extreme point is the image of some primary one.

Proposition 2.16. *Let $\mathcal{W}_1, \mathcal{W}_2 \in \mathcal{E}(A)$ and suppose the extreme point $\boldsymbol{p}$ is the image of the extreme fixed point $\boldsymbol{q}$ under generating maps for both $\mathcal{W}_1$ and $\mathcal{W}_2$. Then relative to their common refinement $\mathcal{W}_1 \circ \mathcal{W}_2$, $\boldsymbol{q}$ remains primary and $\boldsymbol{p}$ is its image under some generating map.*

Proof. If $w^1(\boldsymbol{q}) = w^2(\boldsymbol{q}) = \boldsymbol{q}$ then also $w^1(w^2(\boldsymbol{q})) = \boldsymbol{q}$. Similarly, if $\hat{w}^1(\boldsymbol{q}) = \boldsymbol{p}$, then $\hat{w}^1(w^2(\boldsymbol{q})) = \boldsymbol{p}$. ■

(*d*) *The class of disjoint polyhulled attractors*

Definition 2.17. *An attractor is polyhulled if it has only finitely many extreme points. Figures 7–16, except figure 8, are polyhulled.*

Remarks 2.3. Every flat attractor is polyhulled.

Theorem 2.18. (Refinement) *Let A be a polyhulled attractor. Then there exists $\mathcal{W} \in \mathcal{E}(A)$ such that every extreme point $\boldsymbol{p}$ is the image $\boldsymbol{p} = w(\boldsymbol{q})$ of a primary point $\boldsymbol{q}$ of A under some generating map w. If in addition A is disjoint, then $\mathcal{W}$ can be chosen disjoint also.*

Proof. Let $\mathcal{W}$ be an IFS for A, if A is disjoint, take $\mathcal{W}$ to be disjoint also. Let $\boldsymbol{p}_0 = \boldsymbol{p} \in \mathrm{ext}(A)$. By repeated application of the extreme points theorem, there exists a sequence of extreme points $\boldsymbol{p}_1, \boldsymbol{p}_2, \ldots$, and maps $w_1, w_2, \ldots$ in $\mathcal{W}$ such that

$$\boldsymbol{p}_{i-1} = w_i(\boldsymbol{p}_i), \qquad i = 1, 2, \ldots.$$

But since there are at most finitely many distinct extreme points for polyhulled attractors, the sequence must cycle, i.e. for some non-negative integers j_0 and $k_{\boldsymbol{p}}$,

$$\boldsymbol{p}_j = \boldsymbol{p}_{j+k_{\boldsymbol{p}}}, \qquad j \geqslant j_0.$$

If $k_{\boldsymbol{p}} = 0$, then $\boldsymbol{p}_{j_0}$ is the fixed-point of w_{j_0}. If $k_{\boldsymbol{p}} \neq 0$, consider the composition f

$$f = w_{j_0+1} \circ \ldots \circ w_{j_0+k_{\boldsymbol{p}}}.$$

Clearly $\boldsymbol{p}_{j_0}$ is the fixed-point of f. If $j_0 > 0$ then $\boldsymbol{p}$ itself is not a fixed-point. Instead it is the image

$$\boldsymbol{p} = w_1 \circ \ldots \circ w_{j_0}(\boldsymbol{p}_{j_0}).$$

of the extreme fixed point $\boldsymbol{p}_{j_0}$ under the composition $w = w_1 \circ \ldots \circ w_{j_0}$. Let $k = \max\{k_p, j_0\}$. Then the conclusion holds for this point $\boldsymbol{p}$ for the refinement $\mathcal{W}^k$ of $\mathcal{W}$.

By proposition 2.16, if $\boldsymbol{r}$ is the image of an extreme fixed point of a generating map in $\mathcal{W}$, then it continues to be for $\mathcal{W}^k$ as well. Hence we may continue as above for each extreme point and arrive at a new IFS $\mathcal{W}' \supset \mathcal{W}$ satisfying the requirements of the conclusion. If the original IFS is disjoint, $\mathcal{W}'$ will be also. ■

Corollary 2.19. *Every polyhulled attractor has at least one primary point for some IFS.*

Proof. From the proof of the refinement theorem, $\boldsymbol{p}_{j_0}$ is primary as is every extreme point in the cycle in the refined IFS. ■

Remarks 2.4. In view of this result, the dragontails attractor of figure 10, has an IFS for which the three extreme points (0,0), (1,0), and (0,1) are primary; in fact the cubic refinement $\mathcal{W}^3$, see table 2, contains the map

$$w_1^3(\boldsymbol{x}) = \begin{pmatrix} \frac{1}{8} & 0 \\ 0 & \frac{1}{8} \end{pmatrix}$$

for which $(0,0)$ is fixed.

Definition 2.20. *An affine contraction u is locally invariant for an attractor A if there exists a neighbourhood $\mathcal{N}$ of its fixed point $\boldsymbol{p}$ such that $u(\mathcal{N} \cap A) \subset \mathcal{N} \cap A$ (u is not necessarily part of an IFS for A). A locally invariant map whose fixed point is also an extreme point of A is locally formative. An extreme point $\boldsymbol{p}$ of A is locally primary if it is the fixed point of some locally invariant map for A.*

Theorem 2.21. *Every extreme point of a polyhulled disjoint attractor is locally primary.*

Proof. Let $\boldsymbol{p}$ be such an extreme point. By the construction of the refinement theorem, there is a non-singular affine map w such that $\boldsymbol{p} = w(\boldsymbol{q})$ where $\boldsymbol{q}$ is primary. Let f be an affine map showing $\boldsymbol{q}$ is primary, then $h = wfw^{-1}$ is the required locally invariant map. For if W and F are the linear parts of w and f respectively, $w = W + (\boldsymbol{p} - W\boldsymbol{q})$ and $f = F + (\boldsymbol{q} - F\boldsymbol{q})$, then $h = WFW^{-1} + (\boldsymbol{p} - WFW^{-1}\boldsymbol{p})$. Clearly h has the required properties on any open set containing the w tile of $\boldsymbol{p}$ and disjoint from all other tiles. ■

3. Orbits of two-dimensional affine maps

From theorem 2.21 every extreme point $\boldsymbol{p}$ of an attractor A is the fixed point of some locally formative map f. In this section we draw a correspondence between the eigenvalues and eigenvectors of such a map and the structure of A near $\boldsymbol{p}$. Letting L be the corresponding Jordan form matrix and S the matrix whose columns are the eigenvectors, then the linear part F of f is given by

$$F = SLS^{-1}. \tag{3.1}$$

The translational part of f is then easily determined knowing its fixed point $\boldsymbol{p}$ (see equation (3.2)). Thus a complete list of characterizing information for an affine map consists of (a) its eigenvalues, (b) its eigenvectors, and (c) its fixed point.

Since the eigenvalues of real 2×2 matrices are either both real or are complex conjugates, we may divide the study into four cases: (E_1) the eigenvalues are real and distinct, (E_2) the eigenvalues are equal (hence real) and there are two linearly independent eigenvectors, (E_3) the eigenvalues are equal and there is only one linearly

independent eigenvector, and (E_4) the eigenvalues are complex. As noted in the Introduction, we exclude from consideration here attractors resulting from iterated function systems containing singular maps. A disjoint tile resulting from such a map will be confined to a line segment. Our methods can handle such attractors, but their consideration results in having to deal with many additional special cases which we leave for the reader. Moreover, in the last chapter we show these attractors can be treated as limiting cases of non-singular attractors.

By our definition of extreme point, if the fixed point of a transformation lies on at most one supporting line then it cannot at the same time be an extreme point of the attractor. One of the aims of this section is to characterize, in terms of spectral properties, those maps which can have extreme fixed-points and those which cannot.

(*a*) *Translation simplification*

The general form of a two-dimensional affine transformation ϕ is

$$\begin{pmatrix} r \\ s \end{pmatrix} = \begin{pmatrix} a & b \\ c & d \end{pmatrix} \begin{pmatrix} x \\ y \end{pmatrix} + \begin{pmatrix} e \\ f \end{pmatrix} = F\boldsymbol{x} + \boldsymbol{b},$$

or $\boldsymbol{r} = \phi\boldsymbol{x}$. Here F is the linear part of ϕ and $\boldsymbol{b}$ is the translation. All affine maps ϕ in this work are assumed to be contractive (and hence uniformly contractive),

$$\|\phi\boldsymbol{x} - \phi\boldsymbol{y}\| \leqslant s\|\boldsymbol{x} - \boldsymbol{y}\| \quad \text{for some} \quad 0 < s < 1.$$

By the uniform contraction property, every orbit tends as a geometric series to a unique limit $\boldsymbol{p}$; thus for every $\boldsymbol{x}$,

$$\lim_{n\to\infty} \phi^n\boldsymbol{x} = \boldsymbol{p}.$$

Such a limit point $\boldsymbol{p}$ is by necessity the unique fixed point of ϕ,

$$\phi\boldsymbol{p} = \boldsymbol{p}.$$

In terms of F the fixed point satisfies the equation

$$F\boldsymbol{p} + \boldsymbol{b} = \boldsymbol{p} \quad \text{or} \quad (I - F)\boldsymbol{p} = \boldsymbol{b}, \tag{3.2}$$

from which $\boldsymbol{p}$ can be found since $I - F$ is not singular when F is a contraction. On the other hand, in solving the encoding problem, this equation can be used in the converse way to calculate

$$\boldsymbol{b} = \begin{pmatrix} e \\ f \end{pmatrix}$$

knowing F and $\boldsymbol{p}$.

Now translate the origin to the fixed point $\boldsymbol{p}$. Let $\boldsymbol{x}' = \boldsymbol{x} - \boldsymbol{p}$, and also $\boldsymbol{y}' = \boldsymbol{y} - \boldsymbol{p}$. If $\boldsymbol{y} = \phi\boldsymbol{x}$ then

$$\boldsymbol{y}' = F\boldsymbol{x} + \boldsymbol{b} - \boldsymbol{p} = F\boldsymbol{x} + \boldsymbol{b} - (F\boldsymbol{p} + \boldsymbol{b}) = F(\boldsymbol{x} - \boldsymbol{p}) = F\boldsymbol{x}'.$$

Therefore by so translating, the study of orbits of affine maps is reduced to studying orbits of linear maps; in particular the problem is reduced from six parameters to four, namely a, b, c, d.

In the sequel we assume the translation has been done and dispense with the use of primes to designate translated points. Thus $F\boldsymbol{x}$ and $\phi\boldsymbol{x}$ will be the same.

(*b*) *Orbits in the complex case*

The next result shows that an affine map with complex eigenvalues cannot give rise to a primary point. As a result, we may exclude case (E_4) from further consideration in this section.

Theorem 3.1. *Let* $\boldsymbol{p}$ *be the fixed-point of an affine contraction with linear part* F *and let* Ω *be the orbit of* $\boldsymbol{x} \neq \boldsymbol{p}$. *If the eigenvalues of* F *are complex, then for every half-space* H *containing* $\boldsymbol{p}$, *both* H *and its complement* H' *meet* Ω. *Hence such a map cannot have an extreme fixed-point.*

Proof. Let F be the 2×2 real matrix with complex eigenvalues. For $0 \leqslant \theta \leqslant \pi$ define $\Delta(\theta)$ as follows. Let $\boldsymbol{u}$ be the unit vector at angle θ (from some fixed reference ray through $\boldsymbol{p}$), that is $\arg(\boldsymbol{u}) = \theta$, and let $\boldsymbol{v}$ be the unit vector $F\boldsymbol{u}/\|F\boldsymbol{u}\|$. Note that $\boldsymbol{v} \neq 0$ since 0 is not an eigenvalue of F. Put $\Delta(\theta) = \arg(\boldsymbol{v}) - \theta$ where $\arg(\boldsymbol{v})$ is the angle of $\boldsymbol{v}$ from the reference ray between $-\pi$ and π. Note that $\Delta(\theta) \neq 0$, $0 \leqslant \theta \leqslant \pi$, and $\Delta(\theta) \neq \pi$ for otherwise F would have a real eigenvector. Also note that only angles θ in the range 0 to π need be considered since $F(-u) = -F(u)$ for linear maps.

Assume $\Delta(0) > 0$ the other case being similar. Since $\Delta(\cdot)$ is continuous, and $\Delta(\pi) = \Delta(0)$, its graph is a connected compact subset of the rectangle $[0, \pi] \times [0, \pi]$. Let $m = \min \Delta(\theta)$ and $M = \max \Delta(\theta)$, $0 \leqslant \theta \leqslant \pi$. Then $0 < m \leqslant M < \pi$. That is m is the minimum angle by which F rotates a vector and M is the maximum angle. Now let H be a closed half-space whose boundary, ∂H, contains $\boldsymbol{p}$ and assume $\boldsymbol{x} \in H$, $\boldsymbol{x} \neq 0$, the case $\boldsymbol{x} \in H'$, the complement of H, being similar. We show $F^n\boldsymbol{x}$ must lie in H' for some n. Taking one of the rays of ∂H from $\boldsymbol{p}$ as a reference, let $\{\boldsymbol{x}, F\boldsymbol{x}, \ldots, F^k\boldsymbol{x}\}$ be the initial terms of the orbit of $\boldsymbol{x}$ whose arguments increase but are less than π. Since $\Delta(\theta)$ is bounded below, this segment must be finite as shown. But then $\arg(F^{k+1}\boldsymbol{x}) \leqslant \arg(F^k\boldsymbol{x}) + M < \arg(F^k\boldsymbol{x}) + \pi$. Hence $F^{k+1}\boldsymbol{x} \in H'$. ■

Corollary 3.2. *No map for a flat attractor can have complex eigenvalues.*

The orbits for the complex case spiral in toward the fixed point and conversely, if the orbits spiral, then the eigenvalues are complex (see the dragon attractor, figure 9).

A linear map F may be decomposed into polar form $F = UR$ where U is unitary and R is symmetric (Nagy 1960). Suppose U is a rotation,

$$U = \begin{pmatrix} \cos\theta & -\sin\theta \\ \sin\theta & \cos\theta \end{pmatrix}, \qquad R = \begin{pmatrix} a & b \\ b & c \end{pmatrix},$$

then in some sense the symmetric part, R, attempts to rotate vectors not lying on an eigenmanifold toward its major eigenmanifold in spite of U. Orbits will not be spirals if θ is not too big.

Theorem 3.3. *Let* $F = UR$ *be the polar decomposition of the linear part of the affine contraction* f *and suppose* U *is a rotation. Let* R *have eigenvalues* ν_1 *and* ν_2 *respectively. Then* f *has spiral orbits if and only if*

$$\left(\frac{\nu_1 + \nu_2}{2}\right)^2 \cos^2\theta < \nu_1\nu_2.$$

Proof. Let S be the matrix of normalized eigenvectors of R, then S is a rotation matrix and hence $SUS^{-1} = U$. Thus the change of basis matrix $SFS^{-1} =$

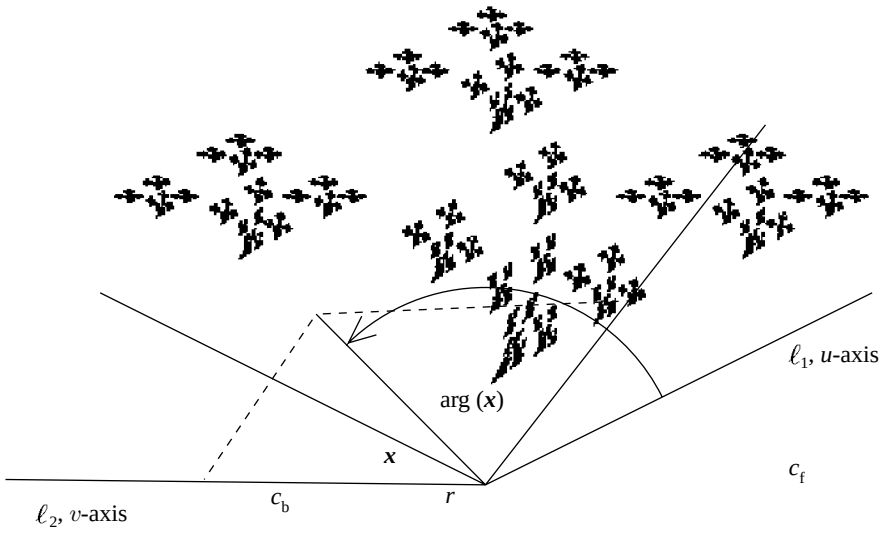

Figure 2. Natural and polar coordinates.

$SUS^{-1}SRS^{-1}$ and is

$$U\begin{pmatrix}\nu_1 & 0\\ 0 & \nu_2\end{pmatrix} = \begin{pmatrix}\nu_1\cos\theta & -\nu_2\sin\theta\\ \nu_1\sin\theta & \nu_2\cos\theta\end{pmatrix}.$$

Hence the characteristic polynomial of F is

$$\lambda^2 - ((\nu_1+\nu_2)\cos\theta)\lambda + \nu_1\nu_2.$$

It follows that the roots are complex if and only if the condition holds. ■

Corollary 3.4. *For a rotational similitude, $\nu_1 = \nu_2$, the condition holds whenever $\theta \neq k\pi$, k an integer.*

Corollary 3.5. *A rotational similitude has at most one supporting line at its fixed point.*

Proof. A rotational similitude whose rotation angle is not equal to π, has complex eigenvalues and in this case the result follows from the theorem. On the other hand, clearly a 180° rotational contraction cannot have more than one supporting line at its fixed point. ■

(*c*) *Natural coordinates*

Let $\boldsymbol{p}$ be an extreme point, let c_f be the ray coincident with the forward (counterclockwise) boundary or limb of the convex hull at $\boldsymbol{p}$ and c_b the ray coincident with the backward limb. We define a local polar coordinate system, (r,θ), at $\boldsymbol{p}$ with r equal to the Euclidean distance of a point $\boldsymbol{x}$ from $\boldsymbol{p}$ and $\theta = \arg(\boldsymbol{x})$ measuring the angle counterclockwise from c_f (see figure 2). In this subsection we define a coordinate system at $\boldsymbol{p}$ by defining unit coordinate vectors $\boldsymbol{e}_1$ and $\boldsymbol{e}_2$ whose definitions depend on the case (E_1)–(E_3).

Let λ_1 and λ_2 be the two real eigenvalues of a locally formative map F (having eliminated case E_4). Since F is a contraction, $|\lambda_1| < 1$, and $|\lambda_2| < 1$. In case E_1, we may assume without loss of generality that $|\lambda_1| \geqslant |\lambda_2|$. By the *major* eigenvalue, λ_1,

we mean the larger in magnitude or, if their magnitudes are equal, the positive one. We refer to λ_2 as the *minor* eigenvalue. Let $\boldsymbol{e}_1$ and $\boldsymbol{e}_2$ be normalized eigenvectors corresponding to λ_1 and λ_2 respectively. Since $-\boldsymbol{e}$ is also an eigenvector if $\boldsymbol{e}$ is, they are determined only up to direction at this point. We will show in the sequel that exactly one ray of the eigenmanifold for λ_1 lies in the exterior of C_A; we take $\boldsymbol{e}_1$ to lie along the other ray, i.e. to point into the convex hull. Take the direction of $\boldsymbol{e}_2$ to be counterclockwise from $\boldsymbol{e}_1$.

In case E_2 the locally formative map is given as $F = \lambda I$ where λ is the common eigenvalue and I is the identity map; that is F is a non-rotational similitude and every non-zero vector is an eigenvector. In this case we take the normalized vectors $\boldsymbol{e}_1$ and $\boldsymbol{e}_2$ to lie along c_{f} and c_{b}, the limbs of the convex hull, respectively. So again $\boldsymbol{e}_2$ lies counterclockwise from $\boldsymbol{e}_1$.

In case E_3, the *geometrical multiplicity one* (or GM-1) case, we will show that one ray of the eigenmanifold lies along the boundary of the convex hull C_A at $\boldsymbol{p}$. As above, let the normalized eigenvector $\boldsymbol{e}_1$ be taken in this direction. Let $\boldsymbol{e}_2$, a pseudo-eigenvector, be chosen perpendicular to $\boldsymbol{e}_1$ of unit length. Let its direction be taken to point into C_A.

In all cases, every point $\boldsymbol{x}$ in the plane has a unique representation

$$\boldsymbol{x} = u\boldsymbol{e}_1 + v\boldsymbol{e}_2, \tag{3.3}$$

for scalars u and v, where v is the projection onto the eigenmanifold of $\boldsymbol{e}_2$ along the direction of $\boldsymbol{e}_1$ and u is the projection onto the eigenmanifold of $\boldsymbol{e}_1$ along the direction of $\boldsymbol{e}_2$. We will refer to these (u, v) coordinates as the *natural* coordinates of $\boldsymbol{x}$ with respect to F.

Now let ℓ_1 and ℓ_2 be the half-lines beginning at $\boldsymbol{p}$ and running parallel to $\boldsymbol{e}_1$ and $\boldsymbol{e}_2$ respectively. We refer to these half-lines as the *eigendirections*. Given a half-line, or *ray*, ℓ, by the notation $\ell \cup -\ell$ we mean the whole line containing ℓ. The *eigenmanifold* of λ_i is the line $\ell_i \cup -\ell_i$, $i = 1, 2$. In terms of the natural coordinates, the plane is divided into four *natural quadrants*, as usual in terms of the signs of u and v.

Let $\boldsymbol{x} = u_0\boldsymbol{e}_1 + v_0\boldsymbol{e}_2$. Then the points $\boldsymbol{x}_n$ of its orbit under a linear map F corresponding to cases (E_1) or (E_2), are given by

$$\boldsymbol{x}_n = F^n\boldsymbol{x} = \lambda_1^n u_0\boldsymbol{e}_1 + \lambda_2^n v_0\boldsymbol{e}_2, \qquad n = 0, 1, \ldots,$$

that is, $\boldsymbol{x}_n$ has the natural coordinates

$$u_n = u_0\lambda_1^n \quad \text{and} \quad v_n = v_0\lambda_2^n. \tag{3.4}$$

The analogous equations for a case (E_3) map is derived in § 3 *f*. Note that $u_0 \geqslant 0$ in cases E_1 and E_2 but it is possible that $u_0 < 0$ in case E_3.

The following is self-evident from equations (3.4).

Proposition 3.6. *The orbit of a point on an eigenmanifold is contained in the eigenmanifold.*

Proposition 3.7. *Let the line ℓ contain a flat attractor A. Then ℓ is an eigenmanifold for every generating map of A.*

Proof. For contradiction, let F be a locally formative map of A for which ℓ is not an eigenmanifold. Let $\boldsymbol{p} \in A$ be the fixed point of F and let $\boldsymbol{x}$ be a point of A distinct from $\boldsymbol{p}$. Then by assumption, neither natural coordinate of $\boldsymbol{x}$ is zero, $u_0 \neq 0$ and $v_0 \neq 0$. Since the orbit of $\boldsymbol{x}$ must also lie on ℓ, the point $\boldsymbol{x}_1 = h\boldsymbol{x}$ is a scalar multiple

of $\boldsymbol{x}$, so for some scalar α,

$$\lambda_1 u_0 \boldsymbol{e}_1 + \lambda_2 v_0 \boldsymbol{e}_2 = \alpha(u_0 \boldsymbol{e}_1 + v_0 \boldsymbol{e}_2).$$

Therefore $\lambda_1 = \lambda_2 = \alpha$. But then F is a pure contraction into $\boldsymbol{p}$ and every line through $\boldsymbol{p}$ is an eigenmanifold, contradiction. ■

In the remainder of this section we examine the orbits occurring in spectral cases (E_1)–(E_3).

(*d*) *Real unequal eigenvalues*

Definition 3.8. *Suppose the eigenvalues to be real and unequal. We distinguish five subcases,* (*a*) *through* (*e*). *First, either* $\lambda_2 = -\lambda_1$ *or* $|\lambda_1| > |\lambda_2|$. *We refer to the possibility* $\lambda_2 = -\lambda_1$ *as subcase* (*a*) *the alternating-similitude case. The latter possibility, the differential contractions, can be further subdivided. Since we have excluded singular maps from consideration,* $\lambda_2 \neq 0$, *so that in the remaining cases,* $|\lambda_1| > |\lambda_2| > 0$. *There are four possibilities,* (*b*) *both eigenvalues are positive, the exponential case,* (*c*) *the major eigenvalue is positive, the minor negative, the alternating exponential case,* (*d*) *the major eigenvalue negative, the minor one positive, and* (*e*) *both eigenvalues negative.*

Proposition 3.9. *If* $|\lambda_1| > |\lambda_2|$ *then the orbit for any point* $\boldsymbol{x}$ *not on the minor eigenmanifold tends asymptotically to the major eigenmanifold. If in addition* $\lambda_1 > 0$ *then the orbit lies on one side of the minor eigenmanifold, otherwise it lies on both sides.*

Proof. If $u_0 \neq 0$, then the ratio

$$\frac{v_n}{u_n} = \left(\frac{v_0}{u_0}\right)\left(\frac{\lambda_2}{\lambda_1}\right)^n \longrightarrow 0 \quad \text{and} \quad n \to \infty.$$

It follows that the orbit tends asymptotically to the u axis. By (3.4), if λ_1 is positive, then the sign of u_n remains the same as that of u_0 for all n. Hence, in the natural coordinate system, the orbit remains on the same side of the v-axis as u_0. Otherwise, for $\lambda_1 < 0$, the sign of u_n alternates with each successive n. ■

Corollary 3.10. *If* $|\lambda_1| > |\lambda_2|$ *and* $\lambda_1 < 0$, *then the orbit can have at most one supporting line at* $\boldsymbol{p}$.

Since we will only be concerned with those cases for which there is more than one supporting line, this result excludes from consideration subcases (*d*) and (*e*).

(i) *Alternating-similitudes:* $\lambda_2 = -\lambda_1$

When $\lambda_2 = -\lambda_1$, the even points, $n = 2k$, of an orbit are given by

$$u_{2k} = u_0(\lambda_1^2)^k \quad \text{and} \quad v_{2k} = v_0(\lambda_1^2)^k, \quad k = 0, 1, \ldots.$$

This is a sequence of points tending to $\boldsymbol{p}$ along the ray through (u_0, v_0). Similarly the odd points tend to $\boldsymbol{p}$ along the ray through $(\lambda_1 u_0, -\lambda_1 v_0)$. These rays form a cone at $\boldsymbol{p}$ and more than one supporting line through $\boldsymbol{p}$ is possible provided the cone has an acute interior angle over all points $\boldsymbol{x} = (u_0, v_0) \in A$.

A map with these properties is a true similitude if and only if the eigenmanifolds are orthogonal, otherwise only alternating points behave in true similitude fashion. In the orthogonal case an orbit gives rise to symmetric trajectories about the major eigenmanifold.

Theorem 3.11. *If $\lambda_2 = -\lambda_1$ then the limbs of the convex hull, c_f and c_b, contain a single orbit.*

Proof. It is easy to see that cones containing orbits nest. ■

Corollary 3.12. *In this case the major eigendirection cannot coincide with c_f or c_b.*

Remarks 3.5. See figure 11, the 3-map pine.

Definition 3.13. *Because of the similarity in the treatment of this case and that of the true similitudes, we use the term extended similitude to refer to the cases $|\lambda_1| = |\lambda_2|$.*

(ii) *Exponential case: $\lambda_1 > \lambda_2 > 0$*

Definition 3.14. *When the eigenvalues are both positive, then the discrete parametric equations for an orbit (3.4), parametrized for $n = 0, 1, 2, \ldots$ can be extended to the real line, $-\infty < n < \infty$. (For emphasis we may use t in place of n.) The resulting parametric equations for the position vector $\boldsymbol{x}_t$ give rise to a continuous curve containing the orbit of $\boldsymbol{x}_0 = (u_0, v_0)$. We call this curve the trajectory of (u_0, v_0) under F. When the minor eigenvalue is negative, the trajectory is taken as the curve parametrized by $-\infty < 2n < \infty$.*

Now eliminate the parameter n from (3.4),

$$\ln(u/u_0) = n \ln(\lambda_1) \quad \text{and} \quad \ln(v/v_0) = n \ln(\lambda_2).$$

Hence

$$\frac{\ln(u/u_0)}{\ln(v/v_0)} = \frac{\ln \lambda_1}{\ln \lambda_2} \equiv 1 - \rho. \tag{3.5}$$

So

$$u = u_0 (v/v_0)^{1-\rho}. \tag{3.6}$$

Proposition 3.15. *Let the eigenvalues of F satisfy $\lambda_1 > \lambda_2 > 0$. Then the trajectory through any point (u_0, v_0), $u_0 \neq 0$, $v_0 \neq 0$, is an exponential curve with exponent $\ln \lambda_1 / \ln \lambda_2$. If all the points of the attractor lie strictly on one side of the minor eigenmanifold, then the attractor has a cusp at $\boldsymbol{p}$.*

Proof. The first conclusion follows from (3.6). If all points of the attractor lie strictly on one side of the minor eigenmanifold, then all orbits will be asymptotic to one ray of the major eigenmanifold. ■

Remarks 3.6. Since (3.6) is single valued, trajectories are either disjoint or identical with the common limit point $\boldsymbol{p}$.

Remarks 3.7. See figure 12, flame.

(iii) *Alternating exponential case*

In case $\lambda_1 > 0$ and $\lambda_2 < 0$, the even orbit points $\boldsymbol{x}, F^2\boldsymbol{x}, \ldots$ work just as above except with effective eigenvalues of λ_1^2 and λ_2^2. The odd orbit points also behave as above but occur on the opposite side of the v axis with squared eigenvalues. Hence in this case there is a cusp at the fixed-point along the positive u axis and consequently multiple supporting lines can exist.

(*e*) *Equal eigenvalues, linearly independent eigenvectors: non-rotational similitude*

Let $\boldsymbol{e}_1$ and $\boldsymbol{e}_2$ be two linearly independent eigenvectors and let λ be their common eigenvalue. Let $\boldsymbol{x} = u_0\boldsymbol{e}_1 + v_0\boldsymbol{e}_2$ be any point. Then $F\boldsymbol{x} = u_0\lambda\boldsymbol{e}_1 + v_0\lambda\boldsymbol{e}_2 = \lambda\boldsymbol{x}$. Hence F is a contraction by λ in each direction in this case, i.e. a non-rotational similitude. The orbits will lie on straight lines through the fixed-point. There are two subcases, $\lambda > 0$ and $\lambda < 0$. In the latter, the orbit lies on both sides of the fixed point and hence there can be at most one supporting line, thus we may eliminate the subcase $\lambda < 0$ from consideration.

(*f*) *Geometrical multiplicity one (GM-1) case:* $\lambda_2 = \lambda_1$

By Jordan canonical form, F can be written as

$$\begin{pmatrix} \lambda & \gamma \\ 0 & \lambda \end{pmatrix} \tag{3.7}$$

for a basis $\boldsymbol{e}_1$, $\boldsymbol{e}_2$ where the former is an eigenvector for the eigenvalue λ and the latter is orthogonal to the first. It may be seen that by choosing $\boldsymbol{e}_2$ directed into the attractor, γ is positive. But since $\boldsymbol{e}_2$ is normalized, γ is not necessarily 1. Now let $\boldsymbol{x}$ be a given vector. If $\boldsymbol{x} = u_0\boldsymbol{e}_1$, then the orbit $\{F^n\boldsymbol{x} = u_0\lambda^n\boldsymbol{e}_1 : n = 0, 1, \ldots\}$ is a geometric sequence along the line through $\boldsymbol{e}_1$. The sequence confines itself to the positive (or negative) side of the u-axis if and only if $\lambda > 0$. Otherwise suppose $\boldsymbol{x} = u_0\boldsymbol{e}_1 + v_0\boldsymbol{e}_2$, $v_0 \neq 0$. Then by trivial induction,

$$F^n\boldsymbol{x} = \lambda^n v_0\boldsymbol{e}_2 + (n\lambda^{n-1}v_0\gamma + \lambda^n u_0)\boldsymbol{e}_1, \quad n = 0, 1, \ldots.$$

In parametric equations

$$\begin{aligned} u_n &= n\lambda^{n-1}v_0\gamma + \lambda^n u_0, \qquad n = 0, 1, \ldots \\ v_n &= \lambda^n v_0. \end{aligned} \tag{3.8}$$

Proposition 3.16. *Orbits of an affine map with equal eigenvalues and only one linearly independent eigenvector tend asymptotically to the major eigenmanifold (the u-axis).*

Proof. Clearly u_n and v_n tend to 0 as $n \to \infty$. Moreover the ratio $|v_n/u_n|$ is given by

$$\left|\frac{v_n}{u_n}\right| = \frac{|v_0|}{|n\gamma(v_0/\lambda) + u_0|}$$

and is $O(1/n)$ (harmonic) for $n \to \infty$. ■

(i) *Geometrical multiplicity one (GM-1) trajectory*

If $\lambda < 0$, then unless $v_0 = 0$ (that is the attractor is flat), $n\lambda^{n-1}v_0$ dominates $\lambda^n u_0$ in (3.8) and this term changes in sign with n. Hence so does u_n. Similarly $v_n = v_0\lambda^n$ changes in sign with n and so for large n, u_n and v_n are opposite signed and alternate in sign. Since the orbit is at the same time asymptotic to the u-axis, it follows that there can be no supporting line at the fixed point and so this possibility is excluded from consideration.

Now suppose $\lambda > 0$ and consider the sign of v_0. If $v_0 > 0$ then from (3.8) both v_n and (for large n) u_n are positive and so the orbit approaches the u-axis from the first quadrant. But if $v_0 < 0$, then both v_n and (eventually) u_n will be negative and now the orbit tends to the u-axis from the third quadrant. Since $\boldsymbol{p}$ is an extreme point,

points of the attractor cannot lie on both sides of any line through $\boldsymbol{p}$ and proves the following.

Proposition 3.17. *The major eigenmanifold must be a supporting line of the attractor in the GM-1 case.*

For $\lambda > 0$, we may consider n to be a continuous variable, $-\infty < n < \infty$, and equations (3.8) as the parametric equations of a curve. From the second equation in (3.8), $n = (\ln v - \ln v_0)/\ln\lambda$. From the first equation,

$$\begin{aligned} u &= \frac{n\lambda^n v_0\gamma}{\lambda} + \lambda^n v_0 \frac{u_0}{v_0} = \frac{nv\gamma}{\lambda} + \frac{u_0}{v_0}v \\ &= \left(\frac{\gamma}{\lambda\ln\lambda}(\ln v - \ln v_0) + \frac{u_0}{v_0}\right)v \\ &= \left[\left(\frac{u_0}{v_0} - \frac{\gamma\ln v_0}{\lambda\ln\lambda}\right) + \frac{\gamma}{\lambda\ln\lambda}\ln v\right]v \\ &= (a + b\ln v)v, \end{aligned} \tag{3.9}$$

where the constants a and b are given by

$$a = \frac{u_0}{v_0} - \frac{\gamma\ln v_0}{\lambda\ln\lambda} \quad \text{and} \quad b = \frac{\gamma}{\lambda\ln\lambda}. \tag{3.10}$$

From (3.8) the slope of the secant line segment joining the origin $(0,0)$ to the point (u,v) is given by

$$\frac{u}{v} = a + b\ln v.$$

Since $b \neq 0$, this slope tends monotonically to $\pm\infty$ as v tends to 0 (for sufficiently small v). Hence, once again, the attractor will have a cusp at $\boldsymbol{p}$ along the major eigenmanifold if all points of the attractor lie strictly above the minor eigenmanifold. Consequently multiple supporting lines are possible in this case.

Remarks 3.8. See figure 12, flame.

(*g*) *Summary*

We collect here some observations of the previous subsections. Coordinates refer to figure 2.

Theorem 3.18. *Let F be a locally formative differential contraction for the two-dimensional attractor A with fixed point $\boldsymbol{p}$. Assume the eigenvalues of F are distinct.*

(a) If A is flat, then it is parallel to an eigenmanifold of F.

(b) If A is not flat, then the major eigenvalue of F is positive, $\lambda_1 > 0$, the major eigenmanifold, ℓ_1, of F meets the deleted convex hull $C_A - \{\boldsymbol{p}\}$ of A, $\arg(\ell_1) \leqslant \arg(c_\mathrm{b})$, and the minor eigenmanifold, ℓ_2 meets at most the boundary ∂C_A of C_A, that is $\arg(\ell_2) = 0$ or $\arg(\ell_2) \geqslant \arg(c_\mathrm{b})$.

Proof. The only undemonstrated assertions are those about the major and minor eigenmanifolds of F. For the major eigenmanifold, suppose the assertion is false. Since the orbit for any $\boldsymbol{x}$ not lying on ℓ_2 tends asymptotically to ℓ_1, points of the orbit of such an $\boldsymbol{x}$ must lie in every positive cone centered at ℓ_1, in particular the cone of half-angle $\frac{1}{2}(\arg(\ell_1) - \arg(c_\mathrm{b}))$. This contradicts that c_b supports A.

For the minor eigenmanifold, suppose not. Then there are points of the attractor

$\boldsymbol{x}$ and $\boldsymbol{y}$ lying on both sides of $\ell_2 \cup -\ell_2$. By the analysis of this section, one will tend to ℓ_1 and the other to the opposite side, $-\ell_1$. Hence the line $\ell_1 \cup -\ell_1$ can be the only supporting line through $\boldsymbol{p}$. This contradicts that $\boldsymbol{p}$ is an extreme point. ■

Corollary 3.19. *Relative to the natural coordinate system at $\boldsymbol{p}$, all points of the attractor have non-negative u coordinate, that is the entire attractor lies on one side of the minor eigenmanifold, the first or fourth quadrants or both.*

Proof. The minor eigenmanifold is a supporting line for the attractor at $\boldsymbol{p}$ and therefore all points of the attractor have either non-negative or non-positive coordinates. Since the positive u axis is inside or on the hull of A, the coordinates are non-negative. ■

Corollary 3.20. *With hypothesis as above, unless ℓ_2 coincides with one of c_f or c_b, A has a cusp at $\boldsymbol{p}$.*

Proof. All points of the attractor have positive u coordinate, and therefore tend asymptotically to ℓ_1. ■

Theorem 3.21. *In every case trajectories are single valued as parametrized by the minor natural coordinate v. Hence the natural coordinate v may be taken as the trajectory parameter, $u = \boldsymbol{t}(v)$.*

The results of this section may be summarized in table 1 which correlates the spectral nature of a map with the geometrical properties of its orbits near its fixed point. Note that only in the cases: alternating-similitude, GM-1, exponential, alternating exponential, and non-rotational similitude can the fixed point also be an extreme point of the attractor.

4. Polar coordinate representations

The most readily accessible trajectory is the one which constitutes the edge or margin of an attractor. In the next section we introduce a tool, the *springbar function*, for finding it. We show that from the resulting polar coordinate plot, enough can be learned to enable the construction of arbitrary trajectories. In this section we lay the groundwork for these plots by calculating the polar coordinate plots for the several spectral cases

In this section we assume that $\boldsymbol{p}$ is the extreme fixed point of the formative or locally formative map F.

In this and subsequent sections we allow the direction of $\boldsymbol{e}_2$ to depend upon the context in such a way that when a point $\boldsymbol{x} \in A$ is chosen, the direction of $\boldsymbol{e}_2$ is selected so that $\boldsymbol{x}$ has non-negative component along $\boldsymbol{e}_2$. Then the natural coordinate v is always non-negative.

(*a*) *Polar representation of trajectories by case*

Initially the eigendirections are unknown, hence it is preferrable to recast the trajectories of § 3 in terms of a local polar coordinate system. Distance r is measured from $\boldsymbol{p}$ and angles θ are measured from the forward limb of the convex hull (see figure 2, § 3 *b*). In this section we obtain the polar form of the trajectory curves for each spectral case. Note that the alternating cases follow their non-alternating counterparts but with the square of their eigenvalues.

Table 1.

eigenvalues	designation	orbital geometry	springbar type
	non-primary		
complex	no primary points	spirals	—
$\lambda_1 < 0$, $\lambda_2 < 0$	no primary points	locally sigmoid	—
$\lambda_1 < 0$, $\lambda_2 > 0$	no primary points	locally convex	—
	extended similitudes		
$\lambda_2 = -\lambda_1$	alternating-similitude	wedge, no cusp	eventually const.
$\lambda_2 = \lambda_1$, 2 e-vect.	non-rot. similitude	wedge, no cusp.	eventually const.
	differential contractions		
$\lambda_1 > 0$, $\lambda_2 > 0$	exponential	cusp/wedge	mono./const.
$\lambda_1 > 0$, $\lambda_2 < 0$	alt. exponential	cusp, no wedge	strictly mono.
	geometrical multiplicity one (GM-1)		
$\lambda_2 = \lambda_1$, 1 e-vect.	harmonic	cusp, no wedge	strictly mono.

(i) *Positive refinement for alternating cases*

Let $\mathcal{W} = \{w_1, w_2, \ldots, w_N\}$ be an IFS for A with a (globally) formative map w_1 whose minor eigenvalue is negative. The partial refinement

$$\mathcal{W}' = \{w_1w_1, w_1w_2, \ldots, w_1w_N, w_2, \ldots, w_N\}$$

is an equivalent IFS for A since $w_1(A) = \bigcup_1^N w_1w_i(A)$. But now the eigenvalues of w_1^2 are both positive. The additional maps, w_1w_i, $i \neq 1$, are decorative. In this way we replace all formative maps in $\mathcal{W}$ having negative minor eigenvalue, by its subtile partial refinement one by one and thereby arrive at an equivalent IFS for the attractor for which the alternating cases do not occur for the formative maps. The resulting IFS is the *positive refinement* of $\mathcal{W}$.

Likewise, one may ignore consideration of the alternating cases for locally formative maps since the spectral types of their squares will match the appropriate globally formative generating map in the positive refinement $\mathcal{W}'$. In this way we no longer have to treat the alternating or extended similitude cases.

In order to obtain a minimal IFS solution, one should discriminate for negative minor eigenvalues. However, from the foregoing it is not necessary to do so. Nevertheless it is possible to test for the alternating cases. We leave the development of these tests to the reader.

In the sequal we will assume this positive refinement has been done and that all eigenvalues are non-negative.

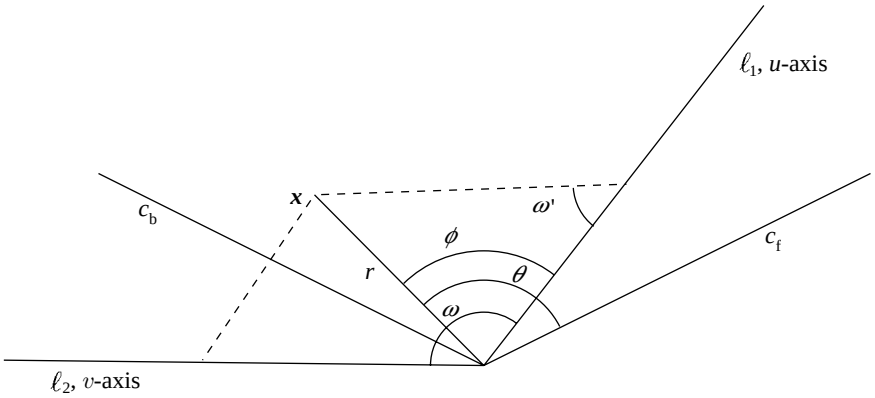

Figure 3. Definition of some angles.

(ii) *Extended similitudes:* $\lambda_2 = \lambda_1$

In this case F is exactly λI with only one unknown parameter, λ. Trajectories of F are rays eminating from the fixed-point $\boldsymbol{p}$ and have the polar form

$$\theta = \text{const.}$$

(iii) *Differential contractions:* $\lambda_1 > \lambda_2 > 0$

In natural coordinates an exponential trajectory is given from equation (3.6) by

$$u = u_0(v/v_0)^{1-\rho}. \tag{4.1}$$

To convert this to polar coordinates, let r be as above and let ϕ measure the angle from ℓ_1 (the u axis), $\phi = |\theta - \arg(\ell_1)|$, $\theta = \arg(\boldsymbol{x})$. Recall from § 3 *d* that ℓ_1 is the trajectory asymptote and therefore is known (see figure 3). Let ω be the angle between the eigenvectors $\boldsymbol{e}_1$ and $\boldsymbol{e}_2$ and let $\omega' = \pi - \omega$ (see figure 3).

By the law of sines

$$\frac{v}{\sin\phi} = \frac{r}{\sin\omega'} \tag{4.2}$$

and by the law of cosines

$$r^2 = u^2 + v^2 - 2uv\cos\omega'. \tag{4.3}$$

Therefore substituting (4.2) into (4.1) gives u in polar coordinates

$$u = \frac{u_0}{v_0^{1-\rho}}\left(\frac{r\sin\phi}{\sin\omega'}\right)^{1-\rho}.$$

Hence equation (4.3) for r becomes

$$r^2 = u_0^2\left(\frac{\sin^2\phi}{v_0^2\sin^2\omega'}\right)^{1-\rho}(r^2)^{1-\rho} + \frac{r^2\sin^2\phi}{\sin^2\omega'} - 2u_0\left(\frac{\sin\phi}{v_0\sin\omega'}\right)^{1-\rho} r^{1-\rho} r\frac{\sin\phi}{\sin\omega'}\cos\omega'.$$

Divide by r^2 $(r \neq 0)$

$$1 = u_0^2\left(\frac{\sin^2\phi}{v_0^2\sin^2\omega'}\right)^{1-\rho} r^{-2\rho} + \frac{\sin^2\phi}{\sin^2\omega'} - \frac{2u_0}{v_0^{1-\rho}}\left(\frac{\sin\phi}{\sin\omega'}\right)^{2-\rho}(\cos\omega')r^{-\rho}.$$

This is quadratic in $r^{-\rho}$

$$u_0^2\left(\frac{\sin^2\phi}{v_0^2\sin^2\omega'}\right)^{1-\rho}(r^{-\rho})^2-\frac{2u_0\cos\omega'}{v_0^{1-\rho}}\left(\frac{\sin\phi}{\sin\omega'}\right)^{2-\rho}(r^{-\rho})+\left(\frac{\sin^2\phi}{\sin^2\omega'}-1\right)=0.$$

Solve for $r^{-\rho}$ by the quadratic formula. It may be verified that the solutions are

$$r^{-\rho}=\frac{v_0^{1-\rho}\sin^{-\rho}\omega'}{u_0\sin^{1-\rho}\phi}\sin(\phi\pm\omega').$$

Since r is always positive (assume ϕ is positive, choose the v axis always on the side of the trajectory), then we must choose the + sign because ϕ can tend to 0. The solution for r is

$$r=\left(\frac{u_0}{v_0^{1-\rho}}\right)^{1/\rho}\sin\omega'\left(\frac{\sin^{1-\rho}\phi}{\sin(\phi+\omega')}\right)^{1/\rho}. \tag{4.4}$$

As ϕ tends to 0 (at the asymptote

$$\frac{\sin^{1-\rho}\phi}{\sin(\phi+\omega')}\longrightarrow\frac{\phi^{1-\rho}}{\sin\omega'}$$

and therefore r tends to

$$r=\frac{\sin\omega'}{\sin^{1/\rho}\omega'}\left(\frac{u_0}{v_0^{1-\rho}}\right)^{1/\rho}\phi^{(1-\rho)/\rho}=\frac{(u_0/v_0^{1-\rho})^{1/\rho}}{(\sin\omega')^{1/\rho-1}}\phi^{1/\rho-1}.$$

Taking logarithms

$$\ln r=\ln\left(\frac{(u_0/v_0^{1-\rho})^{1/\rho}}{(\sin\omega')^{1/\rho-1}}\right)+\left(\frac{1}{\rho}-1\right)\ln\phi \tag{4.5}$$

asymptotically as $\phi\to 0$.

Theorem 4.1. *Let F be locally formative for A at $\boldsymbol{p}$ with distinct eigenvalues, $\lambda_1>\lambda_2>0$. Let ω be the angle between their eigenvectors and let $\rho=\ln\lambda_1/\ln\lambda_2-1$. For any point $\boldsymbol{x}$ of A not lying on an eigenmanifold of F, the graph of $\eta=\ln r$ versus $\xi=\ln\phi$ for the trajectory through $\boldsymbol{x}$ tends asymptotically to a straight line as $\xi\to-\infty$. If m and b are the slope and intercept respectively of this line, then*

$$m=\frac{1}{\rho}-1 \tag{4.6}$$

and

$$e^b=\frac{(u_0/v_0^{1-\rho})^{1/\rho}}{(\sin\omega)^{1/\rho-1}} \tag{4.7}$$

from which ρ and ω can be determined.

Proof. This is a summary of the above. ■

(iv) *Geometrical multiplicity one (GM-1): $\lambda_2=\lambda_1$*

In this case the natural coordinates (u,v) measure distances along, respectively, the asymptote and an axis orthogonal to it. Further the trajectory is given by (3.9)

$$u=(a+b\ln v)v, \tag{4.8}$$

where

$$b = \frac{\gamma}{\lambda \ln \lambda}, \quad \text{and} \quad a = \left(\frac{u_0}{v_0} - \frac{\gamma \ln v_0}{\lambda \ln \lambda} \right). \tag{4.9}$$

Since the asymptote lies along the boundary of the convex hull in this case, ϕ and θ are the same (at least if the asymptote lies along the forward limb of the convex hull).

Change to polar coordinates,

$$v = r \sin \phi$$

and

$$\begin{aligned} r^2 &= v^2 + u^2 \\ &= r^2 \sin^2 \phi (1 + (a + b \ln(r \sin \phi))^2). \end{aligned}$$

Solve for $\ln r$,

$$\frac{\sqrt{(1/\sin^2 \phi - 1)} - a}{b} = \ln r + \ln(\sin \phi).$$

For ϕ near 0 the left-hand side tends to

$$1/b\phi,$$

and the right to $\ln r + \ln \phi$. Hence, asymptotically,

$$\begin{aligned} \ln r &= 1/b\phi - \ln \phi \\ &= \left(\frac{1/b}{\phi \ln \phi} - 1 \right) \ln \phi. \end{aligned}$$

As $\phi \to 0$, $1/\phi \ln \phi \to \infty$. Therefore the graph of $\ln r$ versus $\ln \phi$ does not tend to a straight line; rather its slope tends to $+\infty$.

Theorem 4.2. *In log polar coordinates, the slope of a GM-1 trajectory tends to* $+\infty$ *as* r *(and* ϕ*) tend to 0. Hence this case is distinguished from the exponential case by their respective* $\ln r$ *versus* $\ln \phi$ *graphs.*

5. Springbar function

From the previous two sections we know the character of trajectories for a given type of map. Conversely, from the character of the attractor at an extreme point $\boldsymbol{p}$ we can calculate the locally formative map. In this section we show how to do this up to a single scalar parameter. This is sufficient for calculating a trajectory through a given point.

(*a*) *Supporting trajectories*

Definition 5.1. *By a trajectory family at an extreme point* $\boldsymbol{p}$ *we mean the collection of trajectories* $\boldsymbol{t}_{\boldsymbol{x}_0}(\cdot)$*, one for each initial point* $\boldsymbol{x}_0 \in A$*, corresponding to some locally formative map* F *at* $\boldsymbol{p}$*. Thus a trajectory family is given in natural coordinates by*

$$u = \boldsymbol{t}_{\boldsymbol{x}_0}(v) = u_0 \left(\frac{v}{v_0} \right)^{1-\rho}, \quad v \geqslant 0 \tag{5.1 a}$$

if F is a differential contraction or by

$$u = \boldsymbol{t}_{\boldsymbol{x}_0}(v) = \frac{u_0}{v_0} v, \qquad v \geqslant 0 \tag{5.1 b}$$

if F is an extended similitude or by

$$u = \boldsymbol{t}_{\boldsymbol{x}_0}(v) = (a + b \ln v)v, \qquad v \geqslant 0 \tag{5.1 c}$$

with constants a and b as in § 3 f if F is of geometrical multiplicity one.

Definition 5.2. *By the trace of a trajectory we mean its intersection with the attractor. A trace is complete if it has the extreme point $\boldsymbol{p}$ as a limit point, otherwise it is eventually void.*

Definition 5.3. *The domain of invariance of a trajectory family is the set of points $\boldsymbol{x}_0 \in A$ whose trajectories have a complete trace.*

Definition 5.4. *Let $\boldsymbol{t}_1$ and $\boldsymbol{t}_2$ be two trajectories of the trajectory family at $\boldsymbol{p}$ for $\boldsymbol{x}_1$ and $\boldsymbol{x}_2$ respectively having complete traces. If they lie in the same (natural) quadrant, we say $\boldsymbol{t}_1$ is below $\boldsymbol{t}_2$, $\boldsymbol{t}_1 \prec \boldsymbol{t}_2$, if $\boldsymbol{t}_1(v) \leqslant \boldsymbol{t}_2(v)$, $0 < v < \infty$. Two trajectories lying in different quadrants are not comparable.*

Definition 5.5. *If points of the attractor occupy two natural quadrants, then the supporting trajectory in each is the minimal trajectory with respect to this partial order (see figure 4). If the attractor lies in only one natural quadrant at $\boldsymbol{p}$ with respect to a locally formative map, then the two supporting trajectories are the minimum and the maximum trajectories with respect to this partial order. Treat trajectories lying along the u-axis as the limiting case of trajectories from within the quadrant.*

Remarks 5.9. The supporting trajectory for the lower right-hand frond of the 3-map pine (see figure 11) runs along the frond itself and not along the convex hull since the latter is an eventually void trajectory for this extreme point.

Theorem 5.6. *If the attractor A contains a point lying strictly on one side of the major eigendirection, ℓ_1, of F, then A has a supporting trajectory on that side.*

Proof. Let $\boldsymbol{x}$ be a point of the attractor not lying on ℓ_1, say the v coordinate of $\boldsymbol{x}$ is positive the other case being similar. Let m be a line through $\boldsymbol{x}$ parallel to ℓ_1. For every point $\boldsymbol{a} \in A$ in the first quadrant, let u_a be the point on m where the trajectory through $\boldsymbol{a}$ intersects m. The set of all such u_a is bounded below and so has an infimum, u^*. Then e^*, the trajectory of F through u^*, evidently supports A. It remains to show that e^* is the trajectory of some point of A.

For $\delta = 2^{-n}$ let e_n be a trajectory of A whose intersection u_n with m is within δ of u^*. The mapping which sends $u_n \mapsto e_n$ to its trajectory is a homeomorphism.

Let $\boldsymbol{a}_n$ be the point of A on e_n most distant from the fixed point $\boldsymbol{p}$. The set $\{\boldsymbol{a}_n : n = 1, 2, \dots\}$, as an infinite subset of the compact set A, must have a limit point in A, say $\boldsymbol{a}^*$. Observe that the points $\boldsymbol{a}_n$ are bounded away from $\boldsymbol{p}$. This is because $\boldsymbol{p}$ lies in the secondary tile $F^2(A)$ and since $\boldsymbol{a}_n$ is the most distance attractor point on an orbit, it can't be in $F^2(A)$ as all these points are images under F of some more distant point of A.

Since the points $\boldsymbol{a}_n$ are bounded away from $\boldsymbol{p}$, the limit point $\boldsymbol{a}^*$ is not $\boldsymbol{p}$ and therefore generates an orbit. By the homeomorphism, its trajectory likewise has a limit point on m. But the only one is u^*. Hence the trajectory is exactly e^*. ■

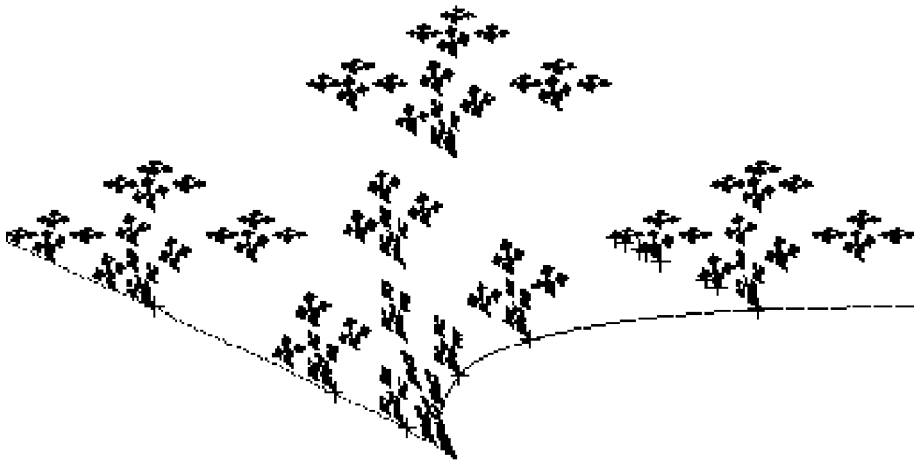

Figure 4. Supporting trajectories.

Definition 5.7. *Let $\boldsymbol{t}^*$ be a supporting trajectory of A at $\boldsymbol{p}$. Its trace will be referred to as a margin of A at $\boldsymbol{p}$.*

(*b*) *Springbar functions*

The most readily accessible trajectory is the one which constitutes the edge or margin of an attractor. In this section we introduce a tool, the *springbar function*, for finding it. We show that from the resulting polar coordinate plot, enough can be learned to enable the construction of trajectory families.

Definition 5.8. *Let $\boldsymbol{p}$ be an extreme point of the attractor A and let $\boldsymbol{p}'$ be the adjacent extreme point on the convex hull C_A counterclockwise from $\boldsymbol{p}$. Let r measure Euclidean distance from $\boldsymbol{p}$ and for each $r > 0$ let $\alpha = \alpha(r)$ be defined by*

$$\alpha = \inf\{\arg(\boldsymbol{x}) \,:\, \boldsymbol{x} \in A \cap \overline{B}_{\boldsymbol{p}}(r)\,\}$$

where $\arg(\boldsymbol{x})$ is measured from the line through $\boldsymbol{pp}'$ to the line $\boldsymbol{px}$ and $B_{\boldsymbol{p}}(r)$ is the ball of radius r around $\boldsymbol{p}$. We refer to the function α so defined as the forward springbar function. It has the following properties: (1) the infimum is attained, (2) α is monotone non-increasing with values from 0 to π, and, due to the use of the closed ball, (3) α is right continuous.

Analogously we define the *backward springbar function* $\beta = \beta(r)$ by

$$\beta = \sup\{\arg(\boldsymbol{x}) \,:\, \boldsymbol{x} \in A \cap \overline{B}_{\boldsymbol{p}}(r)\,\}$$

where $\arg(\boldsymbol{x})$ is measured as above. The properties of β are the same as above except that β is monotone non-decreasing and need not attain the value 0.

The small crosses in figure 4 are points of the attractor upon which the springbar has come to rest.

Put the two together in one plot with α to the right along the positive abscissa and β to the left along the negative abscissa. Either way, r increases away from the origin. We call this the *springbar plot* at $\boldsymbol{p}$.

There is a close connection between the supporting trajectories at $\boldsymbol{p}$ and the forward and backward springbar functions.

Proposition 5.9. *Infinitely many points of the margin on the forward support-*

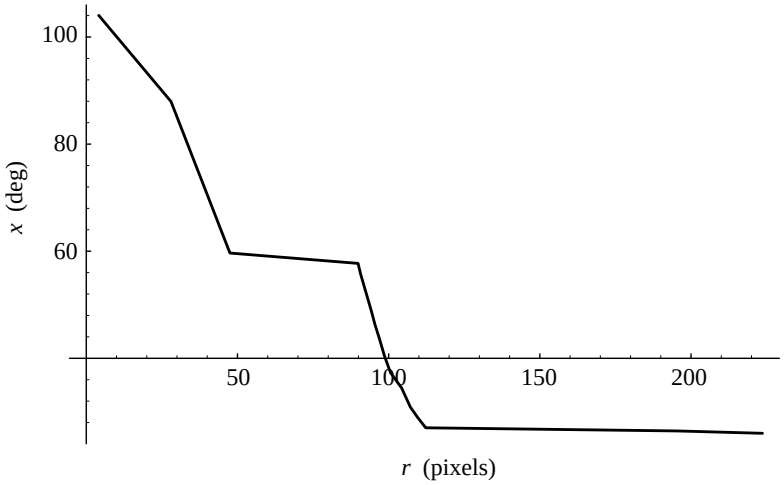

Figure 5. Forward springbar function for figure 4.

ing trajectory lie in the graph of the forward springbar function. Between any two such points, the forward springbar function lies above or on the polar coordinate representation of the forward supporting trajectory. Similar statements hold for the backward springbar function and the backward supporting trajectory.

Proof. Since the supporting trajectory is a trajectory from the domain of invariance, there are attractor points on it inside every deleted ball. By the disjointness of tiles, there is a ball of some positive radius, $r_0 > 0$, such that the only points of the attractor inside this ball also belong to the tile containing $\boldsymbol{p}$. Hence for $r \leqslant r_0$, the springbar will either come to rest on a point of the margin or on a point in the domain of invariance whose trajectory is interior to the supporting trajectory. This proves that the springbar function for $r \leqslant r_0$ lies above or on the polar coordinate plot of the supporting trajectory. On the other hand, since all three types of supporting trajectories are convex, every point of the margin with radius less than r_0 must also lie on the springbar plot. ■

(*c*) *Trajectory family determination*

In this subsection we determine, for the most part uniquely, the trajectory family at an extreme point $\boldsymbol{p}$ by relating the geometry at $\boldsymbol{p}$ to the three spectral cases and the additional subcases resulting from the interplay between the eigenmanifolds and the convex hull. The purpose is to justify the orbital geometry and springbar types columns of table 1 of § 3 *g*.

(i) *Non-rotational similitude:* $\lambda_2 = \lambda_1$

Since the trajectories are rays, in a small enough neighbourhood of $\boldsymbol{p}$ the attractor will be wedge-shaped (see the boughs of the 3-map pine, figure 11). Hence the springbar plot will be two-sided constant if F is globally formative, or two-sided asymptotically constant if F is only locally formative. There will be a jump discontinuity at the origin equal to the interior angle between supporting trajectories at $\boldsymbol{p}$, the wedge angle. The trajectory family in this case is (5.1*b*).

Every direction in this case is an eigendirection, and therefore there are no sub-

cases to deal with here arising from an interplay between the convex hull and the eigenmanifolds.

Note that while the contraction factor of a non-rotational similitude is evident in its orbits, that information is lost in its trajectories, hence the springbar plot cannot determine the contraction factor.

(ii) *Exponential:* $\lambda_1 > \lambda_2 > 0$

There are four subcases here depending on the relationship between the eigenmanifolds and the limbs of the convex hull at $\boldsymbol{p}$: (a) neither coincides with the boundary, (b) ℓ_1 lies on ∂C_A but ℓ_2 does not, (c) ℓ_2 lies on ∂C_A but ℓ_1 does not, or (d) both coincide with the boundary (false similitude case).

If neither eigendirection lies on ∂C_A, the supporting trajectory on each side of ℓ_1 will be an exponential curve (see § 3 *d*); hence there is a two-sided cusp in this case (as in figure 4). The forward springbar function is monotonically decreasing and reaches 0 when r equals the distance to the next extreme point $\boldsymbol{p}'$. As $r \to 0$, $\alpha(r) \to \arg(\ell_1)$ (see figure 5). The backward springbar function is monotonically increasing and tends to the interior angle of the convex hull at $\boldsymbol{p}$. Hence the plot is continuous at the origin.

If the major eigendirection lies on ∂C_A but the minor does not, then that boundary of the hull itself will be a straight line supporting trajectory while on the other side it will be an exponential curve. Hence there will be a cusp at $\boldsymbol{p}$, and consequently the springbar function is constant on one side and monotonic on the other. Again the springbar plot is continuous at the origin in this case. We summarize these facts in the following proposition.

Proposition 5.10. *In subcases* (a) *and* (b) *there is a cusp at* $\boldsymbol{p}$ *and the springbar plot is continuous at the origin,*

$$\lim_{r\to 0}(\alpha(r) - \beta(r)) = 0.$$

If the minor eigendirection lies on ∂C_A *but the major one does not, then again the boundary of the convex hull itself will be a straight line supporting trajectory while the other side will be an exponential curve asymptotically tangent to the major eigendirection. However, this time there will be an asymptotic wedge at* $\boldsymbol{p}$*, instead of a cusp, equal to the angle* ω *between the major and minor eigendirections. The springbar plot will have a jump discontinuity at the origin equal to this angle.*

Proposition 5.11. *In subcase* (c) *there is an exponential wedge at* $\boldsymbol{p}$*,*

$$\lim_{r\to 0}(\alpha(r) - \beta(r)) = \omega > 0,$$

where the wedge angle ω *is the angle between the eigenmanifolds at* $\boldsymbol{p}$*.*

If both eigenmanifolds lie on ∂C_A*, then both supporting trajectories will be the straight lines of the boundary of the convex hull and the springbar functions will be constant with a jump discontinuity at the origin. Unfortunately this is also the signature of an extended similitude case as we have seen above. Therefore we will have to discriminate the two cases in some other fashion than by their springbar plot (see* § 5 *c). We refer to this as the false similitude case.*

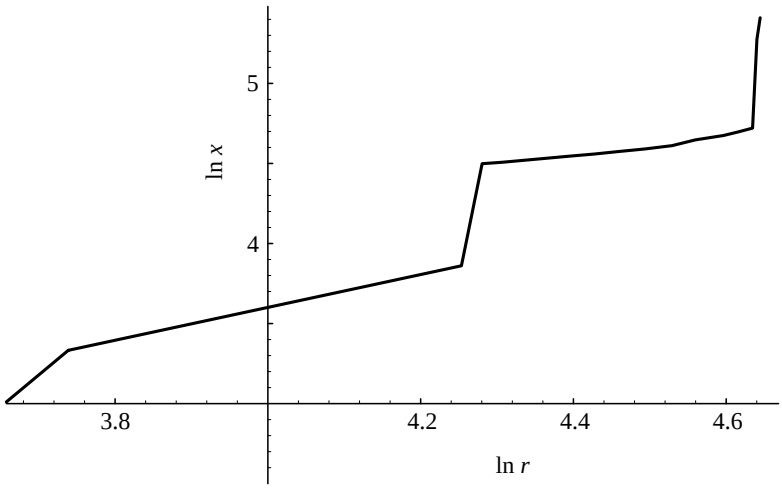

Figure 6. Log-log plot of the springbar function of figure 5.

(iii) *Calculating the trajectory family for an exponential extreme point*

Thus we see that the springbar curve lies above the polar form of the supporting exponential trajectory except where the two have a common value, that is touch. Moreover they touch infinitely often corresponding to a geometric sequence in their minor natural coordinate since every point $\boldsymbol{x}$ lying on such a trajectory, generates an entire orbit contained in that trajectory.

The same will be true of their respective log-log plots. More precisely, since the cusp angle $\arg(\ell_1)$ can be observed in this case, we may form the plot of $\eta = \ln(\arg(\ell_1) - \alpha)$ versus $\xi = \ln r$ for a forward springbar plot (or a plot of $\ln(\beta - \arg(\ell_1))$ versus $\ln r$ for a backward springbar plot) and compare with their supporting trajectory counterpart. From the observations of § 4 *a*, the log-log trajectory plot tends asymptotically to a straight line with slope $M = 1/m$ and intercept $B = -b/m$ to use the notation of equations (4.6) and (4.7) (see figure 6). Moreover the log-log springbar plot lies above the trajectory plot but touches it almost periodically. These considerations yield the following theorem and procedure for calculating the slope M and intercept B.

Theorem 5.12. *For $x < 0$ and $y < \eta(x)$ let $\ell(x, y, M)$ denote the ray on $-\infty < \xi \leqslant x$ through (x, y) and having slope $M > 0$. Let*

$$M(x, y) = \inf\{M \,:\, \ell(x, y, M) \text{ lies below } \eta(\xi), \xi \leqslant x\},$$

and let

$$M(x) = \lim_{y \to -\infty} M(x, y).$$

$M(x)$ is constant for all x, say equal to M^*. Let

$$y(x) = \sup\{y \,:\, \ell(x, y, M^*) \text{ lies below } \eta(\xi),\ \xi \leqslant x\}.$$

Finally let $B(x)$ denote the intercept of the extension of $\ell(x, y(x), M^*)$, then

$$B = \lim_{x \to -\infty} B(x).$$

Proof. By previous results the springbar curve lies above the polar plot and the latter tends to a line. That both limits above exist follows from the observation that the function $M(x, y)$ is monotone in y and the function $B(x)$ is monotone in x. ■

Corollary 5.13. *The parameters m and b of (4.6) and (4.7) are given by*

$$m = \frac{1}{M} \quad \text{and} \quad b = -mB.$$

In turn, the parameters ρ of (5.1a) and the angle ω between the major and minor eigendirections are given by

$$\rho = \frac{1}{m+1} \quad \text{and} \quad \sin\omega = \frac{(u_0 e^{-b\rho})^{1/(1-\rho)}}{v_0}.$$

Hence in this case both eigendirections can be calculated.

Proof. These statements follow from the cited equations. ■

(iv) *Geometrical multiplicity one: GM-1, $\lambda_2 = \lambda_1$*

In this case the single eigendirection lies on ∂C_A (see proposition 3.17) and so the limb of the convex hull on that side will be a straight line supporting trajectory. On the other side there will be a harmonic supporting trajectory. Hence the attractor will have a cusp at $\boldsymbol{p}$.

Having distinguished this case from that of a differential contraction by the unbounded slope in this case of the $\log r$ versus $\log\phi$ springbar plot, theorem 4.2, it remains to solve for the matrix parameters γ and λ, (3.7).

As in the differential contraction case, the springbar plot will lie above the polar coordinate graph of the harmonic supporting trajectory and touch it infinitely often as $r \to 0$. It follows likewise that the natural coordinate (u, v) plot of the springbar function also lies above that of the supporting trajectory. Hence for a given value of v, the springbar value of u exceeds or equals that of the harmonic supporting trajectory (when u exists) and so the springbar plot of $\eta = u/v$ versus $\xi = \ln v$ lies above the corresponding graph of the harmonic supporting trajectory and the two touch infinitely often as $\xi \to -\infty$.

Now the η versus ξ trajectory graph is a straight line. Its slope is given by $b = \gamma/(\lambda \ln\lambda) < 0$ and its intercept is given by $a = u_0/v_0 - b\ln v_0$ (see equation (3.10)). Therefore by fitting a line from below to this η versus ξ springbar plot the parameters a and b can be calculated. We summarize all this in the following theorem.

Theorem 5.14. *In the GM-1 case the unknown parameters a and b may be calculated by fitting a straight line from below to the springbar plot of $\eta = u/v$ versus $\xi = \ln v$.*

Proof. By a procedure similar to that of the differential contraction case (theorem 5.12 above), the negative slope of a tangent line from below can be determined. ■

It follows that here, as in the other cases, enough information is available from the springbar plot to enable the calculation of arbitrary trajectories parametrized by the minor natural coordinate v. In the next section we show how to calculate λ from the pattern of points lying on such a trajectory. Then γ is found from

$$\gamma = b\lambda\ln\lambda. \tag{5.2}$$

(*d*) *Summary*

Theorem 5.15. *With the exception of the false similitude case, trajectories are uniquely determined by the local geometry. That is, the locally formative map is determined to within a scalar parameter such that given an initial point* $\boldsymbol{x}_0$*, the trajectory through* $\boldsymbol{x}_0$ *can be calculated.*

Proof. The existence of a cusp at $\boldsymbol{p}$ implies the locally formative map will be either a differential contraction or GM-1 case. The shape of the cusp uniquely determines which and moreover uniquely determines the trajectory parameters. Except for the false similitude possibility, the absence of a cusp implies a similitude case. ■

Remarks 5.10. See figure 16 for an example of the false similitude case where the locally formative map can be either a differential contraction or a similitude.

6. Gap analysis

The techniques of the last section enable one to calculate trajectory mapping functions for the locally formative map at each extreme point of the convex hull. However, trajectories are not orbits. One scalar parameter separates the two, for instance knowledge of the minor eigenvalue, which, when combined with the trajectory information, completely determines the locally formative map.

Therefore we have reduced the problem to one dimension, and in fact, for one-dimensional attractors, all of which may be interpreted as non-rotational similitudes (see § 1), this section is the starting point for their solution.

A note about flat attractors. Recall that a flat attractor can arise from a two-dimensional IFS when the fixed points lie along a line and an eigenvector of each map is parallel to this line. However, upon encountering a flat attractor, one would proceed to solve it as a one-dimensional attractor.

Throughout this section F will be (the linear part of) either a similitude, differential contraction or harmonic locally formative map at the extreme point $\boldsymbol{p}$. Further assume trajectory maps are parametrized on $0 \leqslant v \leqslant 1$.

(*a*) *Projected trajectory characteristic functions*

Definition 6.1. *Given a trajectory* $\boldsymbol{t}_{\boldsymbol{x}}$ *through* $\boldsymbol{x}$ *we define a one-dimensional fractal subset,* $D(\boldsymbol{t}_{\boldsymbol{x}})$*, of the unit interval as follows. If* F *is a similitude, then* $D(\boldsymbol{t}_{\boldsymbol{x}})$ *is the trace of* $\boldsymbol{t}_{\boldsymbol{x}}$*. If* F *is a differential contraction, then* $D(\boldsymbol{t}_{\boldsymbol{x}})$ *is the projection of the trace of* $\boldsymbol{t}_{\boldsymbol{x}}$ *onto the minor eigenmanifold, that is, letting* P_{ℓ_2} *be the operator in the plane projecting points onto the minor eigenmanifold* $\ell_2 \cup -\ell_2$ *parallel to* ℓ_1*. Put*

$$D(\boldsymbol{t}_{\boldsymbol{x}}) = P_{\ell_2}(A \cap \boldsymbol{t}_{\boldsymbol{x}}).$$

Thus $D(\boldsymbol{t}_{\boldsymbol{x}})$*, the projected fractal dust, is the subset of the minor eigenmanifold consisting of the* v*-coordinates of attractor points on the trajectory* $\boldsymbol{t}_{\boldsymbol{x}}$*.*

Proposition 6.2. *The characteristic function* $\chi_{\mathcal{D}(\boldsymbol{t}_{\boldsymbol{x}})}$

$$\chi_{\mathcal{D}(\boldsymbol{t}_{\boldsymbol{x}})} = \begin{cases} 1, & \text{if } v \in D(\boldsymbol{t}_{\boldsymbol{x}}) \\ 0, & \text{otherwise} \end{cases}$$

is asymptotically 'multiplicatively periodic' for $\boldsymbol{x} \in A$ *in some neighbourhood of* $\boldsymbol{p}$*, that is, for some* $0 < \eta \leqslant 1$ *and some* $\lambda > 0$*,* $\chi_{\mathcal{D}(\boldsymbol{t}_{\boldsymbol{x}})}(v) = \chi_{\mathcal{D}(\boldsymbol{t}_{\boldsymbol{x}})}(\lambda v)$ *for all* $0 < v < \eta$*.*

Proof. Since F is locally formative at $\boldsymbol{p}$, there exists a neighbourhood $\mathcal{N}$ of $\boldsymbol{p}$ invariant under F. Let λ_2 be its minor eigenvalue. For any $\boldsymbol{x} = (u_0, v_0) \in \mathcal{N}$ in natural coordinates, we have $F(\boldsymbol{x}) = (\lambda_1 u_0, \lambda_2 v_0) \in \mathcal{N}$. Hence for v so small that $(\boldsymbol{t}_{\boldsymbol{x}}(v), v) \in \mathcal{N}$ then $\lambda_2 v \in D_{\boldsymbol{t}_{\boldsymbol{x}}}$ if $v \in D_{\boldsymbol{t}_{\boldsymbol{x}}}$. ■

Definition 6.3. *Let $G(\boldsymbol{t}_{\boldsymbol{x}})$ denote the complement of $D(\boldsymbol{t}_{\boldsymbol{x}})$ on $(0, 1]$. Since $D(\boldsymbol{t}_{\boldsymbol{x}})$ is compact and disconnected, $G(\boldsymbol{t}_{\boldsymbol{x}})$ is the countable union of disjoint open intervals, the gaps between the projected fractal dust.*

Definition 6.4. *For $\epsilon > 0$, by the relative ϵ-gaps of trajectory $\boldsymbol{t}_{\boldsymbol{x}}$, we mean the set $G_\epsilon(\boldsymbol{t}_{\boldsymbol{x}}) = \{(a, b) \in G(\boldsymbol{t}_{\boldsymbol{x}}) : b - a = a\epsilon\}$. Let $\mathcal{G}_\epsilon(\boldsymbol{t}_{\boldsymbol{x}}) = \bigcup_{\eta \geqslant \epsilon} G_\eta(\boldsymbol{t}_{\boldsymbol{x}})$ be the set of all gaps of relative size $\boldsymbol{e}$ or larger.*

Due to local invertibility, cf. theorem 2.11, in the vicinity of a fixed point, gaps are transported by a trajectory map F in the same way as points. In particular, there is a dual theory of orbits for gaps just as for points in that a gap along a trajectory is mapped into another gap along the same trajectory by F.

Proposition 6.5. *For at least one $\boldsymbol{e}$, $G_{\boldsymbol{e}}$ is infinite.*

Proof. Let (a, b) be a gap within the neighbourhood of invertibility and let $\boldsymbol{e}$ be such that $(a, b) \in G_{\boldsymbol{e}}$. If λ is a multiplicative period, then for the gap (a', b') where $a' = \lambda a$ and $b' = \lambda b$,

$$b' - a' = \lambda(b - a) = \lambda a\epsilon = \epsilon a' \tag{6.1}$$

and hence belongs to $G_{\boldsymbol{e}}$. By trivial induction, $G_{\boldsymbol{e}}$ is infinite for $\boldsymbol{e}$. ■

Definition 6.6. *Let λ be an asymptotic multiplicative period at $\boldsymbol{p}$, an $\boldsymbol{e}$-gap family started by $g = (a, b)$ is a subset of $G_{\boldsymbol{e}}$ each member $g_k = (a_k, b_k)$ of which is given by $g_k = \lambda^k g$, i.e. $a_k = \lambda^k a$ and $b_k = \lambda^k b$. Note that for a given $\boldsymbol{e}$, the terms of $G_{\boldsymbol{e}}$ need not stem from a single gap family, instead there may be two or even more families represented in $G_{\boldsymbol{e}}$.*

At this point one can calculate the multiplicative period, or contraction factor, λ given an infinite $\boldsymbol{e}$-gap family $G_{\boldsymbol{e}}$. First order the gaps by size, say $g_1, g_2, \ldots$. Now form a triangular matrix whose ijth entry, for $i > j$, is the ordered pair (g_i, g_j). Traverse the table, say along lower left to upper right diagonals, and for each entry (g_i, g_j) in the table calculate

$$\lambda = b_j / b_i.$$

We term such a quotient a *candidate multiplicative period* if and only if also

$$(b_j - a_j)/(b_i - a_i) = \lambda.$$

Definition 6.7. *By the spectrum $\Lambda_{\boldsymbol{x}}$ on the trajectory $\boldsymbol{t}_{\boldsymbol{x}}$ we mean the set of all candidate multiplicative periods λ such that λ^k is also a candidate multiplicative period for $k = 2, 3, \ldots$.*

Proposition 6.8. *Let F have minor eigenvalue λ_2 and be locally invariant on the neighbourhood $\mathcal{N}$ of $\boldsymbol{p}$. Then for every $\boldsymbol{x} \in A \cap \mathcal{N}$, some root, $\sqrt[n]{\lambda_2}$, $n = 1, 2, \ldots$, belongs to $\Lambda_{\boldsymbol{x}}$. Hence λ_2 also belongs to $\Lambda_{\boldsymbol{x}}$ for all such $\boldsymbol{x}$.*

Proof. By the uniqueness theorem 5.15, there can be only one multiplicative period at each $\boldsymbol{p}$. On the other hand, by 'chance,' on any one trajectory there can be points of the attractor which give rise to arbitrary roots of periods (see the cantorrows attractor, figure 15). ■

(*b*) *Locally formative map determination by case*

Let $\boldsymbol{p}$ be an extreme point of A. By the springbar analysis of § 5 applied at $\boldsymbol{p}$, we form a preliminary determination of the spectral type of the locally formative map F at $\boldsymbol{p}$, the possibilities are: (*a*) similitude or false similitude, (*b*) differential contraction, or (*c*) GM-1. With the exception of the false similitude case, the results enable the calculation of true trajectories $\boldsymbol{t}_{\boldsymbol{x}}$ for each point $\boldsymbol{x} \in A$. In the false similitude case the trajectories are wrongly assumed to be rays.

In this section we examine the spectral families case by case and show how to make a complete determination of the locally formative map in each case.

This section is organized according to springbar type, rays, exponential trajectories, and harmonic trajectories. From table 1 of § 3, rays occur in the non-rotational similitude, alternating-similitude, and false-similitude cases. Exponential trajectories occur in the exponential and alternating exponential cases. Recall that through positive refinements, we may assume that the alternating cases do not occur.

(i) *Non-rotational similitude:* $\lambda_2 = \lambda_1$

In this case the locally formative map F is exactly λI and has only the one unknown parameter λ. Note that every direction is an eigendirection. When F is only locally formative, a given trajectory $\boldsymbol{t}_{\boldsymbol{x}}$ either eventually intersects a deleted tile of $\boldsymbol{p}$ or eventually intersects the attractor only at $\boldsymbol{p}$ itself. Therefore by proposition 6.8, every non-empty spectrum will contain the multiplicative period corresponding to the locally formative map F. We summarize this as follows.

Theorem 6.9. *In the case when $\lambda_2 = \lambda_1$ (non-rotational similitude) their common value λ is given by*

$$\lambda = \max \bigcap_{\boldsymbol{x}} \Lambda_{\boldsymbol{x}},$$

where $\boldsymbol{x}$ is taken over the domain of invariance of F.

(ii) *Exponential:* $\lambda_1 > \lambda_2 > 0$

As noted in § 5 *c* (ii) there are four subcases here depending on the relationship between the eigenmanifolds and the limbs of the convex hull at $\boldsymbol{p}$: (*a*) neither coincide with the boundary, (*b*) ℓ_1 lies on $\partial C(A)$ but ℓ_2 does not, (*c*) ℓ_2 lies on $\partial C(A)$ but ℓ_1 does not, or (*d*) both coincide with the boundary (false similitude case). In the first three cases, either the forward, the backward or both supporting trajectories will be exponential curves.

It follows from theorem 5.12 of § 5 *c* (iii) that in these three subcases, either the forward, the backward, or both springbar graphs will correctly identify this case and, by corollary 5.13 of § 5 *c* (iii), allow the calculation of trajectory maps. The solution now proceeds similar to that of the non-rotational similitude case treated in § 6 *b* (i) above. We summarize this as follows.

Theorem 6.10. *In subcases (a), (b), and (c) of the exponential case, the minor eigenvalue λ_2 is given by*

$$\lambda_2 = \max \bigcap_{\boldsymbol{x}} \Lambda_{\boldsymbol{x}}$$

with the intersection taken over all $\boldsymbol{x}$ in the domain of invariance of F. Then the

major eigenvalue is given by

$$\lambda_1 = \lambda_2^{1-\rho},$$

where ρ is calculated from corollary 5.13.

(iii) *False similitude, eigendirections coincide with ∂C_A*

In this case the springbar analysis has a similitude signature and therefore the gap analysis proceeds as if trajectories are rays. It can be shown by example that (*a*) both a differential contraction with its eigendirections lying along the limbs of the convex hull and a similitude can be invariant maps at an extreme point (see the twodcantor attractor, figure 16), and (*b*) that in addition, the similitude can be incomplete in a way we make precise with the concept of residues (see the cantorrows attractor figure 15).

Definition 6.11. *Let w be an attractor invariant map. We call the set $A - w(A)$ the residue of w. If the fixed point $\boldsymbol{p}$ of w is also a limit point of its residue, then we say the residue is asymptotic for w.*

In the false similitude case there are three possibilities: either a similitude or a differential contraction can serve as the solution map at $\boldsymbol{p}$, or only a differential contraction will serve, no similitude is locally invariant at $\boldsymbol{p}$, or finally a similitude is invariant at $\boldsymbol{p}$ but leaves an asymptotic residue.

In the first case our gap analysis will find the similitude solution as usual and there will be no asymptotic residue.

In the second case, the gap analysis will fail in that the intersection of spectra over all rays will be empty, i.e. no similitude is invariant at $\boldsymbol{p}$. Consequently it can be inferred that this is a differential contraction with the eigendirections known (namely being the limbs of the convex hull). It remains to determine the eigenvalues, i.e. contraction factors along the eigendirections. Without knowing these values it is not possible to construct a trajectory map and hence the only spectra available are the two for the eigendirections. Let Λ_{f} and Λ_{b} be these spectra for the forward and backward limbs respectively. On the other hand, these spectra will contain the desired contraction factors. Letting ν_{f} denote the supremum of Λ_{f}, we know that the corresponding eigenvalue λ_{f} is some power of ν_{f}, i.e. $\lambda_{\mathrm{f}} = \nu_{\mathrm{f}}^{n_{\mathrm{f}}}$ for some integral $n_{\mathrm{f}} > 0$. Similarly for the other contraction factor, $\lambda_{\mathrm{b}} = \nu_{\mathrm{b}}^{n_{\mathrm{b}}}$ for some integral $n_{\mathrm{b}} > 0$ where ν_{b} is the supremum of Λ_{b}.

Let $\boldsymbol{n}$ denote the multi-index $(n_{\mathrm{f}}, n_{\mathrm{b}})$. For a multi-index $\boldsymbol{n}$, let $F_{\boldsymbol{n}}$ denote the differential contraction with eigenvalues $\lambda_{\mathrm{f}} = \nu_{\mathrm{f}}^{n_{\mathrm{f}}}$ and $\lambda_{\mathrm{b}} = \nu_{\mathrm{b}}^{n_{\mathrm{b}}}$ and $\Omega_{\boldsymbol{n}}$ denote the domain of invariance of $F_{\boldsymbol{n}}$. Finally let

$$\Sigma = \{(n_{\mathrm{f}}, n_{\mathrm{b}}) \,:\, F_{\boldsymbol{n}}(\Omega_{\boldsymbol{n}}) \text{ has no asymptotic residue}\}.$$

As noted above, Σ is not empty and every multi-index in Σ is a solution. The best solution is the one for which the Jacobian $\det F_n = \lambda_{\mathrm{f}}\lambda_{\mathrm{b}}$ is largest.

In the third case, similitudes can be invariant at $\boldsymbol{p}$ but all leave an asymptotic residue. The solution here proceeds just as in the second case discussed above.

Theorem 6.12. *In the false similitude case there exist contraction factors λ_{f} and λ_{b} such that the locally invariant map w can be constructed.*

(iv) *Geometrical multiplicity one*

By theorem 5.14 the parameter $b = \gamma/\lambda \ln \lambda$ can be calculated from the springbar analysis. Hence given a point $\boldsymbol{x} = (u_0, v_0) \in A$, $a = u_0/v_0 - b \ln v_0$ can be calculated and hence by (3.9) the trajectory through $\boldsymbol{x}$ found. As in the other cases, project its trace onto the minor natural coordinate axis. By equation (3.8) this fractal dust is multiplicatively periodic as in the other cases. Now use the gap analysis as before to calculate the spectrum $\Lambda_{\boldsymbol{x}}$. Then

$$\lambda = \max \bigcap_{\boldsymbol{x} \in A} \Lambda_{\boldsymbol{x}}.$$

Now knowing λ, γ is given by

$$\gamma = b\lambda \ln \lambda$$

and the case solved.

Theorem 6.13. *The GM-1 case can be solved as detailed above.*

7. Encoding image tiles

Given an extreme point $\boldsymbol{p}$, by the techniques of § 4 and § 5, its locally formative map f can be calculated. As in § 5, if the domain of invariance of f is not the entire attractor, then f is not a generating map. This possibility is the subject of the present section. Also we treat the encoding of the maps corresponding to *interior* tiles.

We develop in this section a technique for calculating invariant affine maps carrying a given primary extreme point to a given secondary one all the while preserving eigendirections and supporting trajectories. Of course any such map can be included in an IFS for A. But a solution must also leave no asymptotic residue as well. Only if the primary/secondary pair are correctly matched will such a map be a solution for the secondary point (see below). Hence it may be necessary to exhausitively test for correct matches. This will always succeed since there are at most finitely many primary extreme points (and we are assuming A is an IFS attractor). Note that decorative maps, unlike formative ones (cf. theorem 3.1), can be rotational similitudes.

(*a*) *Encoding secondary tiles*

As in § 2, let $\boldsymbol{p} = w(\boldsymbol{q})$ where $\boldsymbol{q}$ is a primary extreme point and w is a decorative globally invariant map for A; our goal in this section is to calculate w. Assume f is the formative map for $\boldsymbol{q}$, $\boldsymbol{q} = f(\boldsymbol{q})$. Then a locally invariant map h for $\boldsymbol{p}$ is given by $h = wfw^{-1}$. (We invoke here our rank two assumption on the attractor so that w^{-1} always exists.) Our next theorem is well known and notes that the spectral characteristics of f and h are identical.

Theorem 7.1. *Let h, f, and w be as above, and let H, F, and W be their linear parts respectively. Then H and F have identical eigenvalues. Furthermore $\boldsymbol{x}$ is an eigenvector of F if and only if $W\boldsymbol{x}$ is an eigenvector of H.*

By this theorem, the candidate primary extreme points of which $\boldsymbol{p}$ is the image must have identical spectra to that at $\boldsymbol{p}$. If more than one primary extreme point qualifies, then the technique below can be applied to each yielding at least one decorative map w as a solution. Hence assume the primary extreme point $\boldsymbol{q}$ is to be mapped by a decorative map w to the secondary extreme point $\boldsymbol{p}$.

In addition to the correspondence of eigendirections, there is a correspondence of supporting trajectories.

Theorem 7.2. *Let $w \in \mathcal{W}$ be the decorative map at $\boldsymbol{p}$ for $A = A(\mathcal{W})$. If $\boldsymbol{t}^*$ is a supporting trajectory at the pre-image $\boldsymbol{q}$ of $\boldsymbol{p}$, then $w(\boldsymbol{t}^*)$ is a supporting trajectory at $\boldsymbol{p}$.*

Proof. Obviously $w(\boldsymbol{t}^*)$ has a complete trace at $\boldsymbol{p}$. Since affine maps preserve order, no image of a complete trace at $\boldsymbol{q}$ lies beyond that of $w(\boldsymbol{t}^*)$. It follows that if there is a complete trace at $\boldsymbol{p}$ beyond that of $w(\boldsymbol{t}^*)$, it must belong to different tile than $\boldsymbol{p}$ but have $\boldsymbol{p}$ as a limit point. But this is impossible since tiles are closed and disjoint. ■

Hence supporting trajectories go into supporting trajactories under decorative maps. Nevertheless the different spectral cases of the formative maps require different treatments.

(i) *Differential contraction case*

In all three spectral cases we seek the six affine parameters defining a decorative map w. We will use the condition that the primary point $\boldsymbol{q}$ must map to the secondary extreme point $\boldsymbol{p}$ to solve for the translational part of w. Hence the problem is reduced to finding the four elements of the linear part W.

In the differential contraction case we have distinct eigenvalues and eigenvectors to work with, and since by theorem 7.1 these must correspond between the primary and its secondary, the problem is reduced to two parameters. This may be seen as follows. Using the eigenvectors in both the domain and range of w as bases, its linear part diagonalizes to a matrix of the form

$$\Lambda = \begin{pmatrix} g & 0 \\ 0 & h \end{pmatrix},$$

where the parameters g and h stem from the as yet unknown contractions along the eigendirections.

Additionally from theorem 7.2 we know that the supporting trajectories must correspond. Let $u = u_0\lambda_1^t$, $v = v_0\lambda_2^t$ and $r = r_0\lambda_1^\tau$, $s = s_0\lambda_2^\tau$ be the forward supporting trajectories at the primary and secondary extreme points respectively. In these equations t and τ are the independent variables, u, v, r, and s are the natural coordinate dependent variables and all other parameters are known. Mapping the primary trajectory by Λ gives $\begin{pmatrix} r & s \end{pmatrix}^{\mathrm{T}} = \Lambda \begin{pmatrix} u & v \end{pmatrix}^{\mathrm{T}}$ or

$$r_0\lambda_1^\tau = gu_0\lambda_1^t \quad \text{and} \quad s_0\lambda_2^\tau = hv_0\lambda_2^t, \tag{7.1}$$

which holds in the sense that for each t there exists a τ for which both equations hold. In particular this is true for $t = 0$ with some corresponding value τ_0; that is

$$r_0\lambda_1^{\tau_0} = u_0 g \quad \text{and} \quad s_0\lambda_2^{\tau_0} = v_0 h.$$

A similar calculation can be made for the backward supporting trajectory; however, the resulting equation is not independent. Thus we are left with three unknowns but only two equations. Next we show how to calculate one of g or h directly. It follows that the other may be found from (7.1) and the required map solved.

Given $g > 0$ the decorative map, say w_g, will be completely determined. We define

$H(g)$ to be the one-sided Hausdorff set distance from $w_g(A)$ to A, that is

$$H(g) = \sup_{\boldsymbol{b}\in w_g(A)} \inf_{\boldsymbol{a}\in A} \|\boldsymbol{a}-\boldsymbol{b}\|_2$$

(see Shonkwiler 1989).

Evidently $H(g)$ is zero if and only if $w_g(A) \subset A$, that is if and only if w_g is invariant for that particular choice of g. Denote the set of such values by G,

$$G = H^{-1}(0). \tag{7.2}$$

Since w_g is invertible, the set of such points g has no limit point other than the origin.

It remains to satisfy the residue property. If the primary and secondary are correctly matched, then one or more values of $g \in G$ will not have an asymptotic residue. To select out these values, we form the one-sided Hausdorff distance $\mathcal{H}_g$ from the $w_g^{-1}(A \cap w_g(C_A))$ to A, where as usual C_A is the convex hull of A,

$$\mathcal{H}_g = \sup_{\boldsymbol{b}\in w_g^{-1}(A\cap w_g(C_A))} \inf_{\boldsymbol{a}\in A} \|\boldsymbol{a}-\boldsymbol{b}\|_2.$$

As above, this is zero if and only if $w_g^{-1}(A \cap w_g(C_A)) \subset A$, implying w_g leaves no asymptotic residue.

Remarks 7.11. The solution found by the above will not necessarily be the optimal one in terms of having the largest tile.

(ii) *GM-1: harmonic case*

This goes just as above. Using natural coordinates reduces the problem to solving for the diagonal matrix Λ. Matching harmonic supporting trajectories between primary and secondary extreme points reduces the problem to finding one of g or h directly, that is, h becomes a function of g. And one of these, say g, may be determined by assuring both invariance, $w_g(A) \subset A$, and an absence of asymptotic residue, $w_g^{-1}(A \cap w_g(C_A)) \subset A$.

(iii) *Similitude case*

Unfortunately here all rays are eigendirections and consequently there will be no equation stemming from their correspondence. However, using supporting trajectories as the basis for natural coordinates, as we have (cf. § 3 *c*), reduces the problem to solving the diagonal matrix Λ as before.

Before showing how to find suitable values for g and h, note that it will not be known in advance to which secondary supporting trajectory, forward or backward, the forward supporting primary trajectory will map. Hence the following procedure might have to be applied to both possibilities.

As above, to each pair of values (g, h) there will correspond a decorative map, $w_{(g,h)}$, which preserves supporting trajectories. Define again the one-sided Hausdorff distance, $H(g, h)$, from $w_{(g,h)}(A)$ to A, that is

$$H(g,h) = \sup_{\boldsymbol{b}\in w_{(g,h)}(A)} \inf_{\boldsymbol{a}\in A} \|\boldsymbol{a}-\boldsymbol{b}\|_2.$$

Evidently $H(g, h)$ is zero if and only if $w_{(g,h)}(A) \subset A$, that is if and only if $w_{(g,h)}$ is invariant for that particular choice of g and h. Since $w_{(g,h)}$ is invertible, the set of such pairs has no limit point other than the origin. As above, let $G = H^{-1}(0)$.

Again assuming there is a solution for the chosen primary and secondary extreme points, the set of all pairs $(g, h) \in G$ for which the one-sided Hausdorff distance $\mathcal{H}$ from $w_{(g,h)}^{-1}(A \cap w_{(g,h)}(C_A))$ to A is zero is non-empty and any such pair constitutes a solution. The pair with largest product, gh, is the optimal pair to use as it has the largest Jacobian.

Theorem 7.3. *Using the procedure described above of matching primary and secondary extreme points, corresponding eigendirections, corresponding forward or backward supporting trajectories and chosing the parameter g (or the parameters g and h) so that both one-sided Hausdorff distances H and $\mathcal{H}$ are zero calculates a decorative map w which tiles the secondary extreme point.*

(iv) *False similitude case*

Of course if a false similitude primary extreme point is mapped by some decorative map of an IFS to a secondary extreme point, then that secondary extreme point will react to the springbar and gap tests just as primary does. And of course its locally formative solution follows in the same way. Therefore, as above, the match of spectral signatures identifies corresponding extreme points.

Solving the secondary extreme point proceeds exactly as in the similitude case, matching supporting trajectories, and in the final stage, insuring the map be invariant and leaving no asymptotic residue. There are no special problems here.

(*b*) *Encoding interior tiles*

(i) *One-dimensional solution*

The main problem is finding the interior points at which to apply the gap analysis. We will use the gaps themselves for this.†

Theorem 7.4. *Let x be an end point of any gap. Then x is the fixed point of some invertible locally formative map.*

Proof. If C_A is the convex hull of A, then

$$A = \bigcap_{k\to\infty} \bigcup_{i_1,\ldots,i_k} w_{i_1} \ldots w_{i_k}(C_A) \tag{7.3}$$

and hence the set of gaps are given by

$$\bigcup_{k\to\infty} \bigcap_{i_1,\ldots,i_k} [w_{i_1} \ldots w_{i_k}(C_A)]^c$$

in which the intersections are over open intervals. Each resulting intersection is a gap,

$$g = \bigcap_{i_1,\ldots,i_k} [w_{i_1} \ldots w_{i_k}(C_A)]^c$$

any endpoint $\boldsymbol{x}$ of which is an endpoint of one of the sets $w_{i_1} \ldots w_{i_k}(C_A)$. But this composition is the required locally formative map of the theorem, or possibly with further refinement to yield a smaller but strongly disjoint tile. ■

Corollary 7.5. *Any point $\boldsymbol{a} \in A$ which is not a two-sided limit point of A, is the image of an extreme point of A and conversely.*

† The authors thank George Donovan for his discussion of this point leading to the idea.

It has already been noted that the gaps in an attractor (with at least two generating IFS maps) are countable and may be well ordered by length. Since the sets $w_i(A)$, are disjoint compact sets for some IFS $\mathcal{W}$ for A, it follows that there exists a minimum distance $\delta > 0$ between them, cf. proposition 2.4. Now consider the end-points of gaps of length δ or larger. That is, candidate points for the gap analysis in solving interior tiles are the end points of the gaps g as above for which length $g \geqslant \delta$, a finite set, cf. theorem 2.11.

At any point in the solution process, the points of A can be classified into two sets U and R, unresolved and resolved respectively. One might say the points in R are 'coloured'. A point $\boldsymbol{r}$ of the latter are images $\boldsymbol{r} = w(\boldsymbol{a})$ of some point $\boldsymbol{a} \in A$ under some map w determined by the solution process so far. The solution process is done when all points of A are coloured.

Remarks 7.12. By using the refinement theorem and by simplfying to positive refinements, cf. § 4 *a* (i), our ultimate solution will not be the minimal one in terms of number of maps. However, with these two exceptions, our other solution techniques produce the largest map (in terms of eigenvalue) invariant for the attractor at every step.

Of course the largest gap will occur between tiles in any IFS. However, subsequent gaps in the well-ordered list may occur inside tiles. The gap analysis applied to one of these will calculate a subtile that may eventually be discarded.

Theorem 7.6. *Given a disjoint one-dimensional attractor A, the gap solution procedure as detailed above constructs an IFS in finitely many steps whose attractor is A.*

Proof. By the refinement theorem, each extreme point is primary or the image of a primary extreme point and hence is solvable by one map. From above, each interior tile is solvable in a finite number of steps by application of theorem 7.4. ■

(ii) *Two-dimensional solution*

Proposition 7.7. *The affine image of a convex polygon is a convex polygon.*

Proof. This is an easy observation from the fact that an affine map takes half-spaces into half-spaces. ■

Proposition 7.8. *The finite disjoint union of convex polygons is polyhulled.*

Proof. This is an elementary observation. ■

Definition 7.9. *For a given PHD attractor A let Ω denote the collection of all pairs (γ, ϵ) where γ is a simple closed curve lying in A^c and $\epsilon = \operatorname{dist}(\gamma, A)$.*

Consider the relation $(\gamma_1, \epsilon_1) \equiv (\gamma_2, \epsilon_2)$ if and only if γ_1 is homotopically equivalent to γ_2 within A^c. Clearly this is an equivalence relation on Ω and hence divides it into equivalence classes. We exclude from further consideration the null-homotopic curves. For each such equivalence class, Γ, let $\epsilon_\Gamma = \max\{\epsilon : (\gamma, \epsilon) \in \Gamma\}$. The set of maximum epsilons is countable and of course is naturally ordered large to small. In case of ties, and there can be only finitely many ties, any order will suffice.

Theorem 7.10. *Let $\mathcal{W}$ be an IFS for A. The portion of A inside any closed curve as above is the union of tiles of some refinement of $\mathcal{W}$.*

Figure 7. Shrub.

Figure 8. Black spleenwort fern.

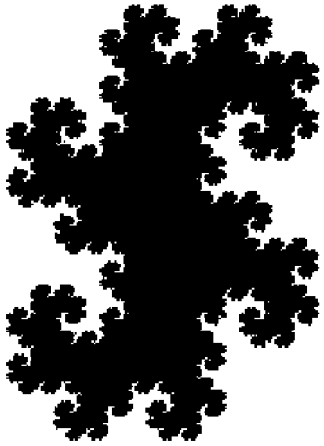

Figure 9. Dragon fractal.

Proof. As $k \to \infty$ the diameter of the tiles of the power refinement $\mathcal{W}^k$ tend to zero. By proposition 2.4 there is a minimum distance $\delta > 0$ separating tiles of the disjoint IFS $\mathcal{W}$. Thus for k sufficiently large so that tile diameter is less than δ it will be that only complete tiles of $\mathcal{W}^k$ will lie inside a given closed curve. ■

Corollary 7.11. *The extreme points of the portion of A inside any closed curve as in the theorem are images of extreme points of A under some affine map.*

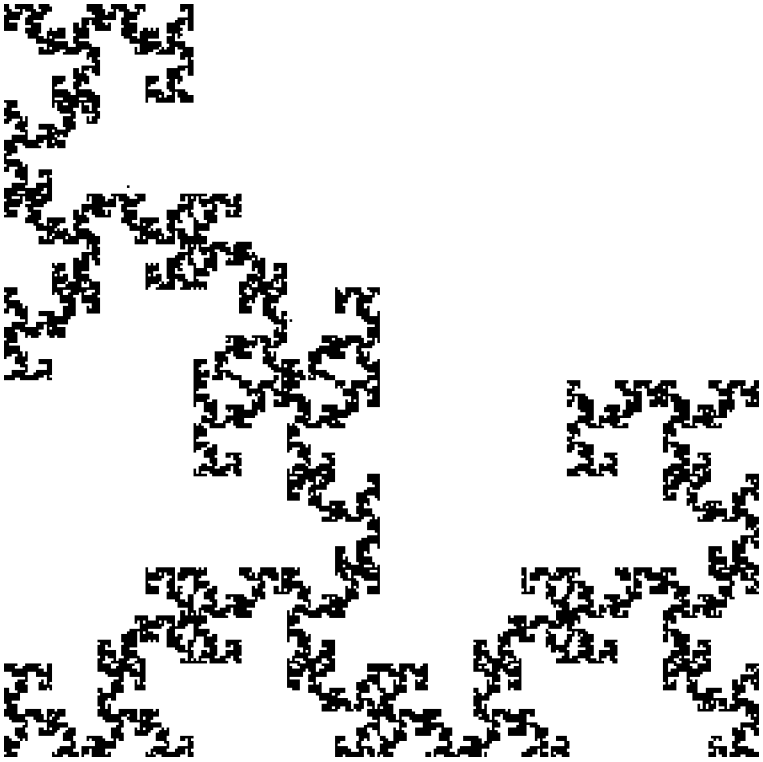

Figure 10. Dragontails.

Proof. By propositions 7.7 and 7.8, the convex hull of such a restriction sub-attractor is polyhulled and by the theorem, its extreme points belong to affine images of tiles of A. But the extreme point of an affine image of a tile, must be the image of an extreme point of the tile. ■

Now solve interior tiles as follows. If the solution of all extreme points leaves no residue, then we are done. Otherwise for each equivalence class Γ starting with the largest max epsilon, solve all the extreme points of the Γ-deleted attractor, namely $A \cap \Gamma^0$ the interior of any $\gamma \in \Gamma$. The solution for the extreme points of this deleted attractor will solve just as secondary extreme points. In finitely many steps, proceeding from large to small max epsilon, the colouring will become complete and the attractor solved.

Theorem 7.12. *Given a disjoint two-dimensional attractor A, the solution procedure as detailed above constructs an IFS in finitely many steps whose attractor is A.*

Proof. This summarizes the entire algorithm as presented in the foregoing several sections. ■

8. Limits of PHD attractors

Many simple IFS fractals are not polyhulled disjoint, for example the 3-map pine of figure 11 and the well-known Sierpinski gasket. Nevertheless these and other just

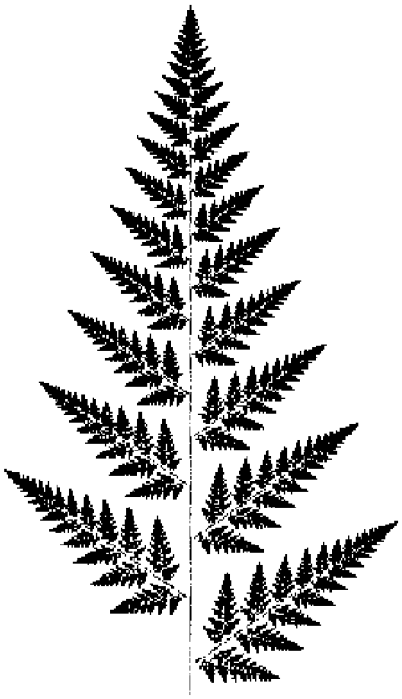

Figure 11. 3-map pine.

Figure 12. Flame.

touching attractors can be solved by our foregoing technique by realizing them as limits of PHD attractors. Also the same holds for attractors due to IFSs having singular maps.

Theorem 8.1. *Let* $\mathcal{W}_n = \{w_1^{(n)}, \ldots, w_r^{(n)}\}_1^\infty$ *be a sequence of iterated function systems each having* r *affine maps. By stringing out the* $6r$ *parameters of these*

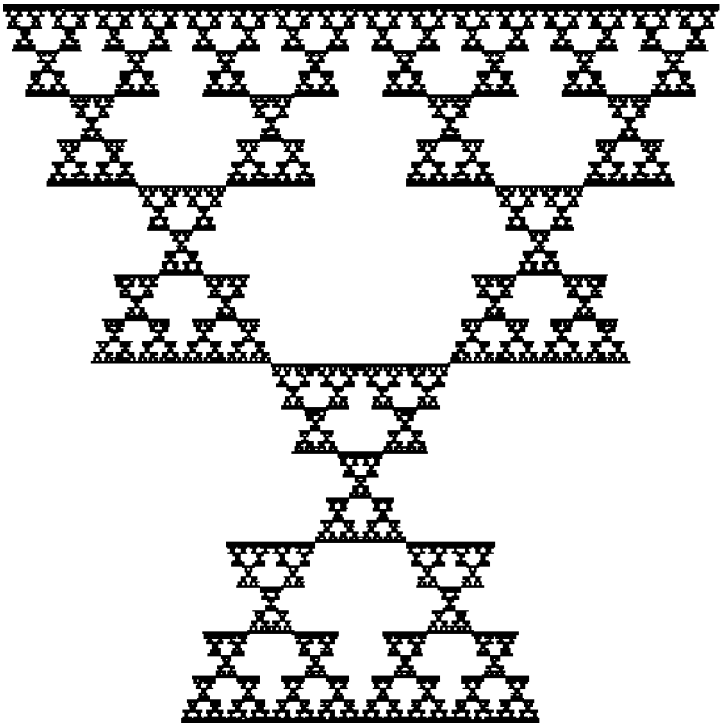

Figure 13. Gasketflip.

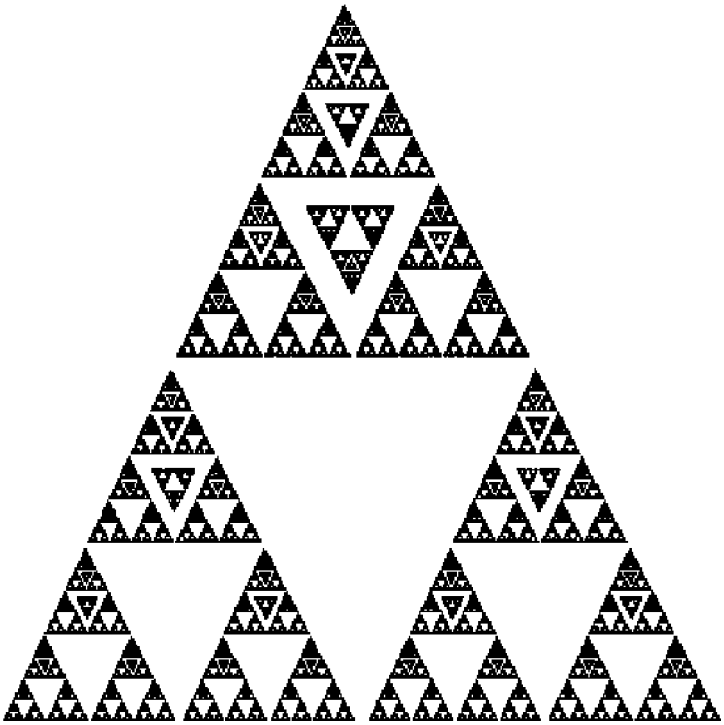

Figure 14. Gasketmod.

PHILOSOPHICAL TRANSACTIONS OF THE ROYAL SOCIETY A MATHEMATICAL, PHYSICAL & ENGINEERING SCIENCES

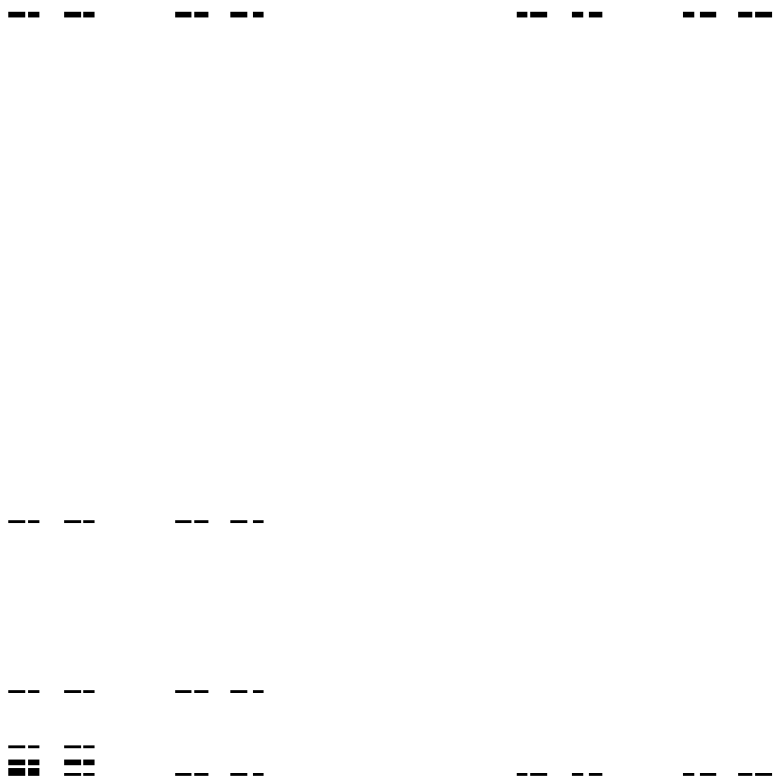

Figure 15. Cantorrows.

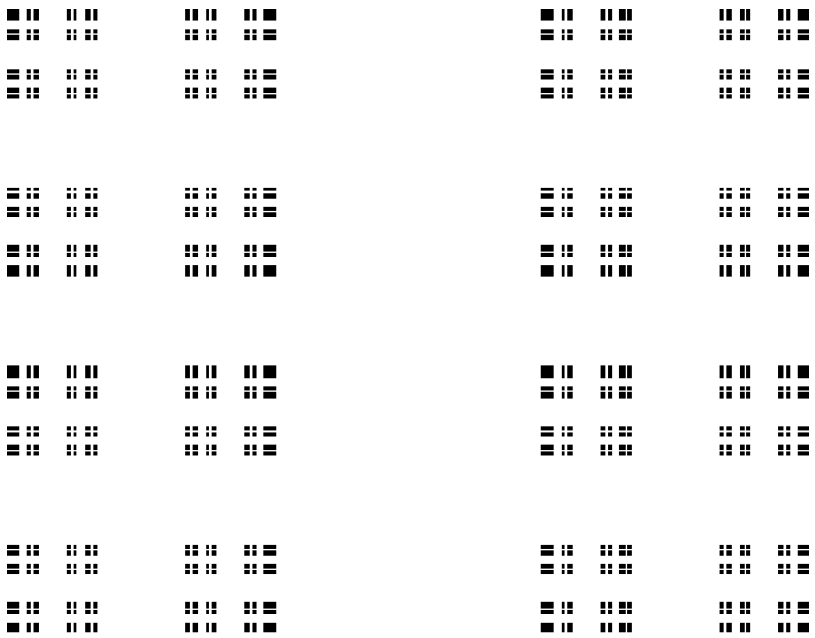

Figure 16. Twodcantor.

maps, each $\mathcal{W}_n$ may be identified with a point, v_n, in 6r-dimensional Euclidean space. Suppose $v_n \to v$ as $n \to \infty$ and $\mathcal{W}$ is the IFS identified with v. Then the sequence of contraction factors s_n of the $\mathcal{W}_n$ converges to s, the contraction factor of $\mathcal{W}$. Further, if $s < 1$, then the sequence of attractors A_n of the $\mathcal{W}_n$ converges to the attractor A of $\mathcal{W}$.

Proof. See Barnsley (1988). ■

Theorem 8.2. *Let $\{A_i\}$ be a sequence of PHD attractors each having an n-map IFS $\mathcal{W}_i = \{w_{i1}, w_{i2}, \ldots, w_{in}\}$ whose tiles $\{w_{ik}(A_i)\}_{i=1}^{\infty}$ converge in the Hausdorff metric on compact subsets of X for $k = 1, \ldots, n$. If the number of their extreme points is bounded, $\mathrm{card}(\mathrm{ext}(A_i)) < M$ for all i, and their contraction factors s_i are bounded away from 1, then:*

(1) the sequence $\{A_i\}$ converges to a set A, whose convex hull is polygonal, and

(2) the sequence of maps $\{w_{ik}\}_{i=1}^{\infty}$ converges to an affine map $w_{\cdot k}$, $k = 1, \ldots, n$, and the set $\mathcal{W} = \{w_{\cdot 1}, w_{\cdot 2}, \ldots, w_{\cdot n}\}$ is an IFS for A.

Proof. Let $A_{ik} = w_{ik}(A_i)$ be the tiles of $\mathcal{W}_i$ and let $A_{\cdot k}$ be their limit as $i \to \infty$ for $k = 1, \ldots, n$. Let $A = \bigcup_{k=1}^{\infty} A_{\cdot k}$. We show $A = \lim_{i \to \infty} A_i$ in the Hausdorff metric.

From the fact that

$$H(A_i, A_j) \leqslant \max_{k=1,\ldots,n} \{H(A_{ik}, A_{jk})\}$$

(see Barnsley 1988) it follows that $\{A_i\}$ is a Cauchy sequence and converges, say to A. First assume A is not flat.

Next we show that the affine images $\{w_{ik}(A)\}_{i=1}^{\infty}$ converge for each $k = 1, \ldots, n$ from which it follows that the affine maps $\{w_{ik}\}_{i=1}^{\infty}$ do likewise. But

$$\begin{aligned} H(w_{ik}(A), w_{jk}(A)) \leqslant\ & H(w_{ik}(A), w_{ik}(A_i)) \\ & + H(w_{ik}(A_i), w_{jk}(A_j)) + H(w_{jk}(A_j), w_{jk}(A)). \end{aligned}$$

For i and j large, the first term is small because the sets A_i and A are close together. The same goes for the last term. The middle term is small by the hypothesis that the tiles form a convergent sequence. Therefore the sequence $\{w_{ik}\}_i$ converges as an affine map, $k = 1, \ldots, n$. But since two-dimensional affine maps can be identified as points in six-dimensional Euclidean space, this sequence of points converges, say to the (identified) affine map $w_{\cdot k}$, $k = 1, \ldots, n$. Further, by holding i fixed in the inequality above and letting $j \to \infty$ we see that

$$w_{\cdot k}(A) = \lim_{i \to \infty} w_{ik}(A) = A_{\cdot k}.$$

It follows that, if the sequence of contraction factors s_i remains bounded away from 1, then A is an attractor with IFS $\{w_{\cdot k}\}_{k=1}^{n}$.

Now suppose A is flat. We may assume without loss of generality that it lies along the x-axis. As above, the images $w_{ik}(A)$ converge as $i \to \infty$, but this no longer implies the maps w_{ik} do. However, they will converge in their parameters corresponding to the x-axis, namely the first column of the matrix part and the first term of the translation part. As we noted previously for flat attractors, their parameters corresponding to the y-axis can be arbitrary. Hence the argument above applies in this case too.

To show that A is polygonal, let $\{E_{ij}\}_{j=1}^{j_i}$, denote the extreme points of A_i, for $i = 1, 2, \ldots$. We may assume without loss of generality that $j_1 = \max_{i \geqslant 1} j_i = M$. By

Table 2.

name	figure	symmetric part a	b	c	rotation	fixed point x	y	remarks
shrub	7	0.6	0	0.667	0	0.5	1	not disjoint,
		0.333	0	0.5	−30	0.68	0.53	but all
		0.333	0	0.5	30	0.22	0.8	tiles
		0.6	0	0.667	0	0.5	0	exposed
black	8	0.85	0.0002	0.84	−2.7	0.72	0.82	not polyhulled
spleenwort		0.3	0	0.3	55	0.46	0.124	
fern		0.3	0	0.36	−55	0.52	0.0.06	
dragon	9	0.707	0	0.707	−45	0.625	0.625	just touching
		0.707	0	0.707	−45	0.375	0.375	attractor
dragontails	10	0.5	0	0.5	90	0.4	0.2	no primary
		0.5	0	0.5	90	0.8	0.4	point
		0.5	0	−0.5	90	0.333	0.667	
3-map pine	11	−0.9	0	0.9	0	0.5	0.98	alternating
		0.3	0	0.36	−55	0.52	0.06	similitude
		0.0002	0	0.16	0	0.5	0	
flame	12	0.335	−0.112	0.783	−26.6	0.5	1	exponential
		0.333	0	0.333	0	1	0.5	and
		0.333	0	0.333	0	0	0.5	harmonic
		0.333	0	0.667	−15	0.5	0.25	trajectories
gasketflip	13	0.5	0	0.5	0	0	0	multiple
		0.5	0	0.5	0	0	1	extreme points
		−0.5	0	0.5	0	0.667	0.5	per tile
gasketmod	14	0.5	0	0.5	0	0.5	1	not
		0.5	0	0.5	0	0	0	strongly
		0.5	0	0.5	0	1	0	disjoint
		−0.125	0	−0.125	0	0.5	0.639	
cantorrows	15	0.333	0	0.111	0	0	0	similitude
		0.333	0	0	0	0	1	invariant
		0.333	0	0	0	1	1	but
		0.333	0	0	0	1	0	residue
		0.333	0	0	0	0	0.333	asymptotic
twodcantor	16	0.333	0	0.333	0	0	0	differential
		0.333	0	0.333	0	0	1	contraction
		0.333	0	0.333	0	1	0	or similitude
		0.333	0	0.333	0	1	1	solve

using a standard diagonalization argument and considering subsequences if necessary we may assume without loss of generality that j_i is constant for i sufficiently large, say equal to J, and the points E_{ij} converge to E_j, $j = 1, \ldots, J$, say, as $i \to \infty$. By considering convex combinations (which are linear) and noting continuity of this representation, we see that the $\{E_j\}_1^J$ contain the extreme points of the limit set $A = \lim_i A_i$. ■

(*a*) *Examples*

Let

$$W_\epsilon = \begin{pmatrix} \frac{1}{2} - \epsilon & 0 \\ 0 & \frac{1}{2} - \epsilon \end{pmatrix}.$$

The 3-map IFS

$$w_1(\epsilon) = W_\epsilon, \quad w_2(\epsilon) = W_\epsilon + \begin{pmatrix} \frac{1}{2} + \epsilon \\ 0 \end{pmatrix}, \quad w_3(\epsilon) = \mathcal{W}_\epsilon + \begin{pmatrix} \frac{1}{4} + \frac{1}{2}\epsilon \\ \frac{1}{2} + \epsilon \end{pmatrix}$$

tends to the Sierpinski gasket as $\epsilon \to 0^+$.

The 4-map IFS consisting of $w_1(\epsilon), w_2(\epsilon)$ from above and

$$w_a(\epsilon) = W_\epsilon + \begin{pmatrix} 0 \\ \frac{1}{2} + \epsilon \end{pmatrix}, \quad w_{\mathrm{b}}(\epsilon) = W_\epsilon + \begin{pmatrix} \frac{1}{2} + \epsilon \\ \frac{1}{2} + \epsilon \end{pmatrix}$$

tends to the solid square.

A.D. was supported partly by NSF Grant DMS-9201304. J.G. was supported partly by NSF Grant DMS-9401352.

References

Abenda, S. & Turchetti, G. 1989 Inverse problems for fractal sets on the real line via the moment method. *Nuovo Cim.* B **104**, 213–227.

Barnsley, M. & Demko, S. 1985 Iterated function systems and the global construction of fractals. *Proc. R. Soc. Lond.* A **399**, 243–275.

Barnsley, M. 1988 *Fractals everywhere*. New York: Academic Press.

Barnsley, M., Ervin, V., Hardin, D. & Lancaster, J. 1985 Solution of the inverse problem for fractals and other sets. *Proc. Natn. Acad. Sci.* **83**, 1975–1977.

Barnsley, M. & Sloan, A. 1985 Image compression by simulated thermal annealing. DARPA proposal.

Berger, M. 1991 Random affine iterated function systems: mixing and encoding. In *Difusion processes and related problems in analysis*, vol. II. *Stochastic flows* (ed. M. Pinsky & W. Wihstutzs). Boston: Birkhäuser.

Bessis, D. & Demko, S. 1990 Stable recovery of fractal measures by polynomial sampling. Preprint, School of Math. Georgia Institute of Technology.

Cabrelli, C. A., Molter, U. M. & Vrscay, E. R. 1992 Moment matching for the approximation of measures using iterated function systems. preprint.

Cabrelli, C. A., Forte, B., Molter, U. M. & Vrscay, E. R. 1992 Iterated fuzzy set systems: a new approach to the inverse problem for fractals and other sets. *J. Math. Analyt. Appl.* **171**, 79–100.

Deliu, A., Geronimo, J., Hardin, D. & Shonkwiler, R. 1991 Dimensions associated with recurrent self-similar sets. *J. Camb. Phil. Soc.* **110**, 327–336.

Demko, S. 1990*a* IFS methods for the inverse fractal problem. Preprint, School of Mathematics, Georgia Institute of Technology.

Demko, S. 1990*b* Approximation of measures by fractal generation techniques. Preprint 30332, School of Mathematics, Georgia Institute of Technology.

Diaconis, P. M. & Shahshahani, M. 1986 Products of random matrices and computer image generation. *Contempory Math.* **50**, 173–182.

Falconer, K. J. 1985 *The geometry of fractal sets.* Cambridge University Press.

Handy, C. & Mantica, G. 1990 Inverse problems in fractal construction: moment method solution. *Physica* D **43**, 17–36.

Hutchinson, J. 1981 Fractals and selfsimilarity. *Indiana Univ. J. Math.* **30**, 713–747.

Mantica, G. & Sloan, A. 1989 Chaotic optimization and the construction of fractals: solution of an inverse problem. *Complex Systems* **3**, 37–62.

Mandelbrot, B. 1982 *The Fractal geometry of nature.* San Francisco: W. H. Freeman and Co.

Nagy, B. Sz. 1960 *Extensions of linear transformations in Hilbert space which extend beyond this space.* New York: Frederick Ungar.

Shonkwiler, R. 1989 An image algorithm for computing the Hausdorff distance efficiently in linear time. *Inf. Proc. Lett.* **30**, 87–89.

Strichartz, R. 1993 A fractal radon inversion problem. Preprint 14853, Mathematics Department, White Hall, Cornell University, Ithaca, NY.

Vrscay, E. R. 1990*a* Moment and collage methods for the inverse problem of fractal construction with iterated function systems. In *Fractal 90 Conf. Lisbon, June 6–8.*

Vrscay, E. R. 1991*b* Iterated function systems: theory, applications and the inverse problem. In *Fractal geometry and analysis* (ed. J. Belair & S. Dubuc) *Proc. of the NATO Advanced Study Institute, Montreal, Canada, 3–21 July 1989*, pp. 405–468. Dordrecht: Kluwer.

Vrscay, E. R. 1991*c* Moment and collage methods for the inverse problem of fractal construction with iterated function systems. *Fractals in the fundamental and applied sciences* (ed. H. O. Peitgen, J. M. Henriques & L. F. Penedo). Elsevier.

Vrscay, E. R. & Roehrig, C. J. 1989 Iterated function systems and the inverse problem of fractal construction using moments. *Computers and mathematics* (ed. E. Kaltofen & S. M. Watt), pp. 250–259. Springer.

Received 23 January 1995; accepted 4 May 1995